PHILOSOPHICAL TRANSACTIONS OF THE ROYAL SOCIETY A MATHEMATICAL, PHYSICAL & ENGINEERING SCIENCES

Viscous Centre Modes in the Stability of Swirling Poiseuille Flow

K. Stewartson, T. W. Ng and Susan N. Brown

Phil. Trans. R. Soc. Lond. A 1988 **324**, 473-512
doi: 10.1098/rsta.1988.0036

Phil. Trans. R. Soc. Lond. A **324**, 473–512 (1988) [473]
Printed in Great Britain

VISCOUS CENTRE MODES IN THE STABILITY OF SWIRLING POISEUILLE FLOW

BY (THE LATE) K. STEWARTSON, F.R.S., T. W. NG† AND SUSAN N. BROWN

Department of Mathematics, University College London, Gower Street, London WC1E 6BT, U.K.

(*Communicated by F. T. Smith, F.R.S. – Received* 20 *October* 1986)

CONTENTS

Centre modes in the neighbourhoods of both branches of the neutral curve are identified for viscous rotating flow in a pipe when the Reynolds number is sufficiently large. Limit equations satisfied by these modes are established, and solutions are computed as functions of the azimuthal wavenumber and one additional parameter, μ say, representing the distance from a neutral curve; these compare favourably with

† Present address: Department of Mathematics, The National University, Kent Ridge, Singapore 0511.

existing calculations of the full equations at large but finite values of R. The question of the attainment of an inviscid limit as $|\mu| \to \infty$ is addressed, and it is shown that the solution on the unstable side of the neutral curve is dominantly viscous. The resulting highly oscillatory viscous modes are examined and are shown to be present throughout the region bounded by the neutral curve. It is anticipated that the results may have application in the study of vortex breakdown.

1. Introduction

The linear stability of vortex flows, both inviscid and viscous, has attracted considerable interest over the past few years in the expectation that such studies may lead to greater understanding of the phenomenon of vortex breakdown. This study concerns the normal modes of Poiseuille flow in a rotating pipe at large values of the Reynolds number. Pedley (1968, 1969) showed that circular Poiseuille flow was destabilized by the rotation, and constructed modes in which the disturbance was distributed throughout the width of the pipe in the situation where the ratio of the axial to azimuthal wavenumber was small. He demonstrated instability when R, the Reynolds number based on the maximum unperturbed axial velocity and the radius of the pipe and defined here in §2, was larger than 83, and the results are valid for rotation rates that are not too small. Numerical solutions of the viscous equations for small rotation rates were obtained by Mackrodt (1976) who suspected that the turbulent bursts observed experimentally in the theoretically stable Poiseuille flow were due to residual swirl in the incoming flow.

Inviscid wall modes for swirling Poiseuille flow were obtained by Maslowe & Stewartson (1982) for large values of the azimuthal wavenumber n. These asymptotic modes have the disturbance concentrated in the neighbourhood of the pipe wall near which there is a critical layer. The results were compared with earlier calculations of Maslowe (1974) at finite n, and the conclusion is that the growth rate does not increase with n but achieves a maximum at n approximately equal to four. This asymptotic study for rotating Poiseuille flow has a parallel when the basic flow is an unbounded trailing-line vortex, though in this situation the rotation is stabilizing rather than destabilizing. In that case the large azimuthal wavenumber eigensolutions are ring modes and have been studied by Leibovich & Stewartson (1983) who also obtain a sufficient condition for the instability of a general columnar vortex. This paper did not include an analysis of the neutral points; these have recently been examined by Stewartson & Capell (1985) and by Stewartson & Leibovich (1987).

The modes to be studied here have the maximum disturbance concentrated near the axis of the pipe and are therefore centre modes, in contrast with those described above. In their extensive study of the linear stability of rotating pipe flow at finite values of the Reynolds number R and rotation rates Ω (equivalent to R/ϵ, ϵ being a Rossby number), Cotton & Salwen (1981, hereafter referred to as C.S.), showed that as R increases the near-neutral modes in their calculation become centre modes. This phenomenon seems to occur near *both* branches of their neutral curves in an (R, Ω)-plane. As R becomes large one branch, 'the upper', is distinguished by $\epsilon n \approx \alpha$ (α the axial wavenumber) and the lower by $\epsilon^2/R = O(1)$. Inviscid centre modes with $\epsilon n \approx \alpha$ and $\epsilon \gg 1$ have previously been discussed by Stewartson & Brown (1984), who attempted to trace their development from the modes introduced by Pedley as α/n increased from the values required for the validity of that theory. It is viscous modes that are of interest here however, with particular emphasis on the question whether the inviscid centre modes of Stewartson & Brown are in any sense limits of the centre modes encountered by C.S. as the

Reynolds number of their calculation takes on large but finite values. The connection between the viscous-stability and inviscid-stability characteristics of a flow is worth establishing to promote a proper understanding of the evolutionary process of a flow field. For although the inviscid characteristics are easier to calculate and might be expected to dominate this process when the Reynolds number is large, it is always necessary to enquire if the inviscid property is the limit of a viscous property as the Reynolds number becomes infinite, and if so whether the two are sufficiently close at a reasonable value of R for the inviscid result to be accepted as sufficiently accurate in a particular problem. We shall find that in the case of these centre modes the inviscid limit is *not* invariably attained; indeed when the flow is unstable the inviscid limit is a possibility but it is not the dominant limit at large Reynolds number.

The plan of this paper, which involves examination of both branches of the neutral curve, is as follows. In §2 we describe the geometry, define the parameters of the problem and give the linearized stability equations solved by C.S. These equations contain the four prescribed parameters α, n, ϵ, R, of which n is to be an integer, and the eigenvalue ω which is to be determined so that the homogeneous sixth-order system has a non-trivial solution. In §3 the centre-mode equations for the neighbourhood of the 'upper' branch, $\epsilon n \approx \alpha$, of the neutral curve, are obtained. In these equations the number of parameters is reduced from four to two, namely n and μ, of which the latter measures a scaled distance from the neutral curve. These equations are to be solved over an infinite range of a scaled radial variable s, for these centre modes are, as noted by C.S., independent of the position of the wall. Analytic solutions are obtained for small $|\mu|$ and for large $|\mu|$, the latter of which are, in the limit $|\mu| \to \infty$, the inviscid centre modes of Stewartson & Brown. These analytic solutions are then compared with results from C.S., and from additional data kindly supplied by Professor Salwen, at various large values of the Reynolds number R for the case of $\alpha = n = 1$. It is verified that their modes are indeed becoming functions of the parameter μ alone as R increases, i.e. they are centre modes, and their numerical solutions and the asymptotic solutions of the limit equations are in good agreement for small $|\mu|$ and for large negative μ (the stable side of the neutral curve). However, for large positive μ (the unstable side) the asymptotic solution, for the mode that is least stable at $\mu = 0$, becomes neutral as $\mu \to \infty$ with an eigenfunction that exhibits a critical layer, whereas the results of C.S. indicate an increasing growth rate and a non-singular eigensolution. To resolve this lack of agreement, numerical solutions of the limit equations at finite values of μ are undertaken with particular attention being paid to the values $n = 1$ and 2. The value of unity for n is special in that it is unique in allowing for a non-zero radial velocity at the axis so that particles on the axis at any instant may be deflected from it; such 'bending' modes are described for the analogous trailing-line vortex by Leibovich *et al.* (1986) who show that, in certain circumstances, they can support solitons which may contribute to the transfer of turbulence developed in a zone of agitated fluid. The outcome of the numerical integrations for finite μ is that the asymptotic expansion for $|\mu| \ll 1$ is confirmed, as is the inviscid limit for $\mu \ll -1$. However, for $\mu \gg 1$ the most unstable mode does not assume the inviscid form, but confirms the increasingly unstable trend predicted from the results of C.S. On the other hand, when $n = 1$ the mode that at $\mu = 0$ is the second least-stable mode attains the inviscid limit, and when $n = 2$ the third mode does so. The eigenfunctions of the modes that remain viscous as μ increases are quite different from those of the modes that become inviscid. They are highly oscillatory with the region of oscillation spreading out and moving away from $s = 0$ as μ increases; in contrast, the oscillatory region of the inviscid mode becomes concentrated in the neighbourhood of the critical layer the existence of which is quite evident at values of μ as low

as 50. For the viscous modes the appropriate parameter is $\mu^{\frac{1}{3}}$ so the asymptotic form is not established until μ is considerably larger.

Before analysing the asymptotic form of these viscous modes, which thus dominate the near-neutral inviscid modes of Stewartson & Brown (1984), we present, in §4, a similar study to that of §3 but for the 'lower' branch of the neutral curve where $\epsilon^2/R = O(1)$. There are again two parameters of the centre-mode equation: n and σ, which is analogous to μ. These equations have also been obtained by Berry & Norbury (1985) who solve them for $n = 1$ to find the value of σ for neutral stability. We confirm their value of 6.5 for this but we are more interested in solutions for $\sigma \gg 1$ for which an inviscid limiting form for the equations is also possible. Analytic solutions for small $|\sigma|$ have not been found in this case. Comparison with the results of C.S. taken from data at various large values of R again shows no agreement of the most unstable mode with the proposed inviscid asymptotic form. Numerical solutions of the centre-mode equations at finite values of σ show a phenomenon similar to that which occurs in the upper branch problem. This time, when $n = 1$ the first two modes do not attain the inviscid limit but the third does; when $n = 2$ it is the fourth mode that attains the proposed asymptote. The unstable viscous modes are similar to those encountered near the upper branch.

In §5 we present an analysis for these highly oscillatory increasingly unstable viscous modes, and obtain an asymptotic form that is in good agreement with the numerical solutions of §§3 and 4 at finite but large values of μ and σ. Comparison with the numerical solutions is deferred until §7, because in §6 we show that both upper and lower branch problems become identical as μ, σ respectively increase. This means that these oscillatory eigensolutions persist right across the unstable region of the (R, Ω)-plane of C.S. That the region of validity of these modes might in fact extend from one branch of the neutral curve to the other was suggested to us by Professor F. T. Smith, F.R.S., during the course of the investigation.

In addition to the establishment of these unstable viscous modes two other points of interest have arisen from this study. The first is that an inviscid solution, even when it exists as a limit solution of a system of equations, may not in fact be attained as $R \to \infty$. Secondly, the eigenvalue to be found is not necessarily an analytic function of the parameters of the equation; indeed this property does not hold for any of the cases discussed here. The important eigensolutions are the viscous ones and, although their large amplitudes and steep gradients eventually violate the assumptions under which the equations were linearized, they do confirm the extreme instability of this rotating flow. An examination of their presence or otherwise in unbounded vortices, in particular in the trailing-line vortex of Lessen *et al.* (1974), would be of interest as in that instance, contrary to the example studied here, the swirl is stabilizing.

2. The setting of the problem

We take r_0 to be the radius of the pipe and choose a set of cylindrical polar coordinates $(r_0 X, r_0 r, \theta)$ with $0X$ along the axis so that the pipe boundary is defined by $r = 1$. The basic flow of the incompressible fluid is steady with azimuthal velocity $\Omega_0 r_0 r$ and Poiseuille axial velocity $\epsilon r_0 \Omega_0 (1-r^2)$, ϵ being the Rossby number. We define $R = \epsilon r_0^2 \Omega_0/\nu$, where ν is the kinematic viscosity, to be the Reynolds number of the basic flow and, to compare with the results of C.S., we set $\Omega = R/\epsilon$. The fluid is subjected to a small disturbance in which the components of the velocity and of the pressure respectively take the form

$$[\bar{F}, \mathrm{i}\bar{G}, \bar{H}; \rho\bar{P}) \exp(\mathrm{i}\alpha X - \mathrm{i}n\theta - \mathrm{i}\Omega_0 \omega T), \tag{2.1}$$

where ρ is the density, α is a real positive constant and n a positive integer, while ω is a constant to be found. The reason for taking α to be positive is that earlier studies have indicated that $\alpha n \geqslant 0$ for instability. We do not here consider $n = 0$ because the criterion of Howard & Gupta (1962) for stability of the basic flow to axisymmetric disturbances is violated only if $\epsilon > 2$. The four quantities $\bar{F}$, $\bar{G}$, $\bar{H}$, $\bar{P}$ are functions of r only. After a direct substitution into the Navier–Stokes equations (see also Lessen & Paillet 1974) we find that

$$\alpha r\bar{F}+r\bar{G}'+\bar{G}-n\bar{H}=0 \tag{2.2a}$$

from the equation of continuity, and

$$\gamma\bar{F}-2\epsilon r\bar{G}+\alpha\bar{P}=\frac{\epsilon}{\mathrm{i}R}\left[\bar{F}''+\frac{1}{r}\bar{F}'-\left(\alpha^2+\frac{n^2}{r^2}\right)\bar{F}\right], \tag{2.2b}$$

$$\gamma\bar{G}+2\bar{H}-\bar{P}'=\frac{\epsilon}{\mathrm{i}R}\left[\bar{G}''+\frac{1}{r}\bar{G}'-\frac{n^2+1}{r^2}\bar{G}-\alpha^2\bar{G}+\frac{2n\bar{H}}{r^2}\right], \tag{2.2c}$$

$$\gamma\bar{H}+2\bar{G}-\frac{n}{r}\bar{P}=\frac{\epsilon}{\mathrm{i}R}\left[\bar{H}''+\frac{1}{r}\bar{H}'-\frac{n^2+1}{r^2}\bar{H}-\alpha^2\bar{H}+\frac{2n\bar{G}}{r^2}\right], \tag{2.2d}$$

respectively, from the (X, r, θ) components of the momentum equation, where a prime denotes differentiation with respect to the appropriate independent variable, in this case r, and

$$\gamma = \alpha\epsilon(1-r^2)-\omega-n. \tag{2.3}$$

The appropriate boundary conditions are that

$$\bar{F}=\bar{G}=\bar{H}=0 \quad \text{at} \quad r=1, \tag{2.4}$$

while $\bar{F}$, $\bar{G}$ and $\bar{H}$ are smooth at $r = 0$. The requirement of regularity of $\bar{F}$, $\bar{G}$ and $\bar{H}$ at $r = 0$ with $\bar{G}(0) = 0$, $n > 1$, but $\bar{G}'(0) = 0$ if $n = 1$, is sufficient to ensure that the boundary conditions derived and discussed by Batchelor & Gill (1962) are satisfied. In the event of viscous effects being small over the majority of the range $0 \leqslant r \leqslant 1$, the conditions at $r = 1$ may be replaced by

$$\bar{G}=0 \quad \text{at} \quad r=1, \tag{2.5}$$

with an error $O(\alpha R)^{-\frac{1}{2}}$ due to boundary-layer effects near the wall of the pipe.

The numerical studies of C.S. for finite α, n (typically $\alpha = n = 1$†) strongly suggest that when $R \gg 1$ there are neutral modes in the neighbourhood of $\epsilon n = \alpha$ and where $\epsilon^2/R = O(1)$. For sufficiently large R their neutral curves, drawn in an (R, Ω)-plane for fixed values of n and α, essentially have as the upper branch the straight line $\epsilon n = \alpha$ and as the lower branch the parabola $\epsilon^2/R = \text{const}$. They interpreted these modes as centre modes in that the disturbance was increasingly concentrated near the axis and the position of the wall was of little importance. For the neutral mode that occurs in the neighbourhood of $\epsilon n = \alpha$ the authors make a comparison with Pedley's (1969) theory of the viscous stability of such flows when $\epsilon \ll 1$, $|\alpha| \ll 1$, and R, n and α/ϵ are finite. The comparison is good not only when these conditions are satisfied but also in certain circumstances when they are not. Pedley's theory does not assume that the eigenfunctions are centre modes and indeed his representation of them by three Bessel functions of real argument in a combination that must satisfy the boundary conditions on the pipe would suggest that they should, even when $\epsilon n \approx \alpha$, be termed wall modes.

† Cotton & Salwen's notation is slightly different from that adopted here. The sign of n is changed in (2.1) and they then set $\alpha = -1$, $n = 1$. Their temporal dependence $e^{\sigma T}$ is related to ours through $\omega_r = \sigma_i$, $\omega_i = \sigma_r$.

In the following sections we confirm that the near-neutral modes of C.S. in the neighbourhoods of both branches of the neutral curves in the (R, Ω)-plane become centre modes when $R \gg 1$. This confirmation is achieved by considering the branches separately and undertaking a limiting procedure that in each case reduces the number of parameters from four to two, one of which is the azimuthal wavenumber n. As the second of these parameters increases, possible limiting forms are the inviscid solutions of Stewartson & Brown (1984), although it emerges that in general these are not attained and the dominant limiting eigensolutions are viscous in origin.

3. The neighbourhood of $\epsilon n = \alpha$

Because the numerical results of C.S. indicate strongly that the eigenfunctions in the neighbourhoods of the upper branches of their neutral curves are centre modes we make the scaling

$$r = (\alpha R)^{-\frac{1}{4}} s \tag{3.1}$$

and we shall also assume that

$$\omega = \alpha\epsilon - n + \alpha^{\frac{3}{2}} R^{-\frac{1}{2}} \Lambda n^{-1}, \quad \epsilon = \alpha/n + \mu\alpha^{\frac{5}{2}} R^{-\frac{1}{2}} n^{-1}, \tag{3.2}$$

where s, Λ, μ are $O(1)$ and $R \gg 1$. Thus μ represents a scaled distance from the curve $\epsilon = \alpha/n$ and will be shown to assume a finite non-zero value μ_0 when neutral stability is attained. The unstable side of the curve is described by $\mu > \mu_0$ and the stable side by $\mu < \mu_0$. In addition, Λ replaces ω as the complex eigenvalue to be found.

Then a formal solution of (2.2) may be written down as an asymptotic series, in descending powers of $R^{-\frac{1}{2}}$, of which the leading terms are

$$\left.\begin{aligned} \bar{F} = \alpha^{\frac{3}{4}} R^{-\frac{1}{4}} F_1(s) + O(R^{-\frac{3}{4}}), \quad \bar{G} = G_1(s) + O(R^{-\frac{1}{2}}), \\ n\bar{H} - (r\bar{G})' = \alpha^{\frac{3}{2}} R^{-\frac{1}{2}} s F_1(s) + O(R^{-1}), \\ n\bar{P} - 2r\bar{G} = \alpha^{\frac{5}{4}} R^{-\frac{3}{4}} P_1(s) + O(R^{-\frac{5}{4}}), \end{aligned}\right\} \tag{3.3}$$

and satisfy the differential equations

$$\left.\begin{aligned} (s^2 + \Lambda) F_1 - P_1 + 2\mu s G_1 &= \mathrm{i}\left[F_1'' + \frac{1}{s} F_1' - \frac{n^2}{s^2} F_1\right], \\ (s^2 + \Lambda) G_1 - 2sF_1 + P_1' &= \mathrm{i}\left[G_1'' + \frac{1}{s} G_1' - \frac{n^2+1}{s^2} G_1 + \frac{2}{s^2}(sG_1)'\right], \\ (s^2 + \Lambda)(sG_1)' + \frac{n^2 P_1}{s} &= \mathrm{i}\left[(sG_1)''' + \frac{1}{s}(sG_1)'' - \frac{n^2+1}{s^2}(sG_1)' + \frac{2n^2}{s^2} G_1\right]. \end{aligned}\right\} \tag{3.4}$$

It is convenient to eliminate the reduced pressure P_1 in (3.4) which attain a certain amount of symmetry if we define

$$F_1 = sK_1/n \tag{3.5}$$

so that

$$s^2(\Lambda+s^2)(sK_1'+K_1+nG_1)+2n\mu s^2(sG_1)'$$
$$=\mathrm{i}[s^3K_1'''+4s^2K_1''-(n^2-1)sK_1'+(n^2-1)K_1+ns^2G_1''+3nsG_1'-n(n^2-1)G_1], \quad (3.6a)$$

$$s^2(\Lambda+s^2)(sG_1'+G_1+nK_1)+2n^2\mu s^2G_1$$
$$=\mathrm{i}[s^3G_1'''+4s^2G_1''-(n^2-1)sG_1'+(n^2-1)G_1+ns^2K_1''+3nsK_1'-n(n^2-1)K_1]. \quad (3.6b)$$

We note that as a result of the transformations (3.2) and (3.3), followed by the limiting process $R\to\infty$, the number of parameters has been reduced from four to two, namely n and μ. The procedure may be regarded as successful if, for integer n and given finite value of μ, a value of Λ can be found such that (3.6) have a solution in which G_1 and K_1 are regular at $s=0$ and vanish as $s\to\infty$. For general μ this is a numerical problem and a description of the numerical method of solution we used and the results are presented in §3.4. In the limits $\mu\to 0$ and $|\mu|\to\infty$ analytic solutions are obtainable, however, and we first discuss (in §3.1) those available in the neighbourhood of $\mu=0$.

3.1. *The analytic solutions for small values of* μ

When $\mu=0$ the centre-mode equations (3.6) have two sets of eigenfunctions that may be found exactly. They are obtained by exploiting the symmetry of (3.6a, b) in this limit for which purpose we define

$$K_1+G_1=M, \quad K_1-G_1=N \quad (3.7)$$

and add and subtract the equations which results in

$$s^2(\Lambda+s^2)[sM'+(1+n)M]+2n\mu s^2(sG_1)'+2n^2\mu s^2G_1$$
$$=\mathrm{i}[s^3M'''+(4+n)s^2M''-(n^2-3n-1)sM'-(n-1)(n^2-1)M], \quad (3.8a)$$

$$s^2(\Lambda+s^2)[sN'+(1-n)N]+2n\mu s^2(sG_1)'-2n^2\mu s^2G_1$$
$$=\mathrm{i}[s^3N'''+(4-n)s^2N''-(n^2+3n-1)sN'+(n+1)(n^2-1)N]. \quad (3.8b)$$

The first family of solutions with $\mu=0$ has $N=0$. To derive them we set $M=s^{-n-1}Q$ in (3.8a) and then set

$$Q'=\bar{Q}\,\mathrm{e}^{-\frac{1}{3}\beta s^3}, \quad \beta=\mathrm{e}^{-\frac{1}{4}\mathrm{i}\pi} \quad (3.9)$$

with the result that

$$s^2\bar{Q}''-[2\beta s^3-(1-2n)s]\bar{Q}'-[(2-2n)\beta s^2+1-2n+\beta^2\Lambda s^2]\bar{Q}=0. \quad (3.10)$$

The values of Λ are now chosen so that $\bar{Q}$ is a polynomial whose first term is s^{2n-1}. The values of Λ for this to be possible are

$$\Lambda=-2(2p+n)/\beta \quad (p=0,1,2,\ldots) \quad (3.11)$$

and the eigensolutions M_p corresponding to the first three values of p are

$$\left.\begin{aligned} M_0 &= s^{-n-1}\left\{1-\mathrm{e}^{-\frac{1}{2}\beta s^2}\sum_n\right\}; \quad \Lambda = -2n/\beta, \\ M_1 &= s^{-n-1}\left\{1-\mathrm{e}^{-\frac{1}{2}\beta s^2}\left(\sum_n + 2(\tfrac{1}{2}\beta s^2)^n/n!\right)\right\}; \quad \Lambda = -2(2+n)/\beta, \\ M_2 &= s^{-n-1}\left\{1-\mathrm{e}^{-\frac{1}{2}\beta s^2}\left(\sum_n + 4(\tfrac{1}{2}\beta s^2)^{n+1}/(n+1)!\right)\right\}; \quad \Lambda = -2(4+n)/\beta, \end{aligned}\right\} \tag{3.12}$$

where

$$\sum_n = \sum_{j=0}^{n-1} (\tfrac{1}{2}\beta s^2)^j/j!. \tag{3.13}$$

We note that $M_p = O(s^{n-1})$ as $s \to 0$, and that $M_p = O(s^{-n-1})$ as $s \to \infty$, an algebraic decay that in fact persists for all values of μ and makes the numerical work of §3.4 more difficult.

When $\mu = 0$ and $M = 0$ the second family of eigenfunctions is associated with the same values of Λ as in (3.11) except that p cannot now be zero. The first two are

$$\left.\begin{aligned} N_1 &= s^{n-1}\mathrm{e}^{-\frac{1}{2}\beta s^2}; \quad \Lambda = -2(2+n)/\beta; \\ N_2 &= s^{n-1}\mathrm{e}^{-\frac{1}{2}\beta s^2}(1-\beta s^2/n); \quad \Lambda = -2(4+n)/\beta. \end{aligned}\right\} \tag{3.14}$$

It is possible at this stage to make direct comparison with the solutions of the full equations (2.2) made available to us by Professor Salwen. From this data we have extracted the values of ω, with $\alpha = n = 1$, $\epsilon = 1$ and $R = 10^4$, obtained by using a matrix of order 30, for the five lowest eigenvalues. These are:

$$\begin{array}{c} \omega \\ -0.01424 - 0.01426\mathrm{i} \\ -0.04242 - 0.04253\mathrm{i} \\ -0.04270 - 0.04233\mathrm{i} \\ -0.06841 - 0.06944\mathrm{i} \\ -0.07068 - 0.07050\mathrm{i}. \end{array}$$

The trend evident there, namely the existence of a single eigenvalue followed by higher ones in pairs, may be distinguished in the S-data for all values of R greater than about 10^3. The single eigenvalue corresponds to the eigenfunction M_0 and $p = 0$ in (3.11), and the other two pairs correspond to M_1 and N_1 with $p = 1$, and to M_2 and N_2 with $p = 2$.

The knowledge of the analytic form of these double eigenvalue points is of assistance in initiating the numerical solutions of (3.6) for non-zero μ. Additional terms in the expressions for small μ may be obtained if required, and for the leading mode we have

$$\Lambda = -2n\,\mathrm{e}^{\frac{1}{4}i\pi} - n\mu + \Lambda_2\mu^2 + O(\mu^3), \tag{3.15}$$

where

$$\Lambda_2 = -\mathrm{e}^{-\frac{1}{4}i\pi}(\tfrac{1}{24}\pi^2 - \tfrac{1}{4}) \quad \text{when} \quad n = 1, \tag{3.16}$$

and

$$\Lambda_2 = -\mathrm{e}^{-\frac{1}{4}i\pi}(\tfrac{1}{6}\pi^2 - \tfrac{5}{4}) \quad \text{when} \quad n = 2. \tag{3.17}$$

In terms of the original eigenvalue ω this means that if $n = 1$

$$\omega = \alpha^2 - 1 - 2\,\mathrm{e}^{\frac{1}{4}i\pi}\alpha^{\frac{3}{2}}R^{-\frac{1}{2}} + \alpha^{-1}(\alpha^2-1)(\epsilon-\alpha) + \mathrm{e}^{\frac{3}{4}i\pi}\alpha^{-\frac{7}{2}}R^{\frac{1}{2}}(\tfrac{1}{24}\pi^2 - \tfrac{1}{4})(\epsilon-\alpha)^2 + O(R(\epsilon-\alpha)^3), \tag{3.18}$$

and if $n = 2$

$$\omega = \tfrac{1}{2}(\alpha^2-4) - 2\,e^{\frac{1}{4}i\pi}\alpha^{\frac{3}{2}}R^{-\frac{1}{2}} + \alpha^{-1}(\tfrac{1}{2}\alpha^2-1)\,(2\epsilon-\alpha) + e^{\frac{3}{4}i\pi}\alpha^{-\frac{7}{2}}R^{\frac{1}{2}}(\tfrac{1}{12}\pi^2-\tfrac{5}{8})(2\epsilon-\alpha)^2 + O(R(2\epsilon-\alpha)^3) \tag{3.19}$$

provided, in each case, that $R(n\epsilon-\alpha)^3$ is small.

For the second and third eigenvalues given by $p = 1$ and 2 in (3.11) it is necessary to take appropriate linear combinations of M_1, N_1 and M_2, N_2 respectively. With an $O(\mu)$ correction the eigenvalues (four in all) given to leading order by $p = 1$ and 2 in (3.11) are

$$\Lambda = -2\,e^{\frac{1}{4}i\pi}(2p+n) \pm \mu n^{\frac{3}{2}}(n^3+p)^{-\frac{1}{2}} + O(\mu^2) \tag{3.20}$$

though it has not been confirmed whether this formula also holds for higher values of p. There is no term $O(\mu^{\frac{1}{2}})$ in (3.20) as there are two independent eigenfunctions associated with the double eigenvalue at $\mu = 0$.

When $|\mu|$ is large the numerical solutions to be described in §3.4 indicate that the eigenfunctions take one of two possible limiting forms, and we discuss next the more straightforward of these in which the limit is inviscid.

3.2. *The inviscid limit when* $|\mu| \gg 1$

It emerges that there are two possible limiting forms of solution when $|\mu| \gg 1$, one of which is essentially inviscid and is appropriate when $\mu \ll -1$. When $\mu \gg 1$ this limit is also an analytical possibility and we shall find that it can also be achieved numerically, but that it does not correspond to the most unstable modes which are dominated by the viscosity. The inviscid modes are, to leading order, of the same structure as those of Stewartson & Brown (1984) as $R \to \infty$, and $(\epsilon n-\alpha)/\epsilon n \to 0$, in that order.

When $|\mu|$ is large the natural scaling is to assume that $s^2 = O(|\mu|)$ and $\Lambda = O(|\mu|)$ in which case the right-hand sides of (3.6) are of order $|\mu|^{-2}$ relative to the left-hand sides. The implication then is that the modes are inviscid. We now apply a consistency check on this conjecture by using it to evaluate the two leading terms in the asymptotic expansion of Λ in descending powers of μ. For the leading term we obtain, from (3.6*b*),

$$-nK_1 = (sG_1)' + \frac{2n^2\mu G_1}{\Lambda+s^2} + O(\mu^{-2}G_1) \tag{3.21}$$

and then, from (3.6*a*),

$$s^2G_1'' + 3sG_1' + \left[1-n^2-\frac{4n^2\mu s^2}{(\Lambda+s^2)^2}\right]G_1 = 0 \tag{3.22}$$

of which the solution regular at the origin is

$$G_1(s) = \frac{s^{n-1}}{(\Lambda+s^2)^q}F\left(a, b, n+1, \frac{-s^2}{\Lambda}\right), \tag{3.23}$$

where F is a confluent hypergeometric function and q, a and b are defined by

$$\Lambda = -n^2\mu/q(q+1), \quad a = -q, \quad b = n-q. \tag{3.24}$$

The expression for $G_1(s)$ given in (3.23) has the correct, $O(s^{-n-1})$, algebraic decay if b is chosen to be a negative integer or zero. If, for example, $b = 0$ then G_1 has the simple form

$$G_1(s) = \frac{s^{n-1}}{[s^2 - n\mu/(n+1)]^n} \tag{3.25}$$

and $\Lambda = -n\mu/(n+1)$. If $b = -1$ then

$$G_1(s) = \frac{s^{n-1}}{(s^2 - n^2\mu/(n+1)\,(n+2))^{n+1}}\left(s^2 + \frac{n^2\mu}{(n+1)\,(n+2)}\right) \tag{3.26}$$

and $\Lambda = -n^2\mu/(n+1)\,(n+2)$. The hypergeometric function reduces to a polynomial in s^2 of degree $(-b)$ to give the successive modes.

The correction to the formula (3.24) for Λ is $O(\mu^{-1})$ and may be obtained by substituting the leading approximations to G_1, K_1 into the right-hand sides of (3.6) and requiring that the new differential equations have a solution that is regular at $s = 0$ and vanishes as $s \to \infty$. This condition leads to

$$\Lambda = -\frac{n\mu}{n+1} + \frac{2(n+1)\,(n+2)^2}{2n+3}\frac{\mathrm{i}}{\mu} + O(\mu^{-3}) \tag{3.27}$$

for the modes to which (3.25) is the leading approximation, and

$$\Lambda = \frac{-n^2\mu}{(n+1)\,(n+2)} + \frac{2(n+1)\,(n+2)\,(n^3+10n^2+24n+12)}{n^2(2n+5)}\frac{\mathrm{i}}{\mu} + O(\mu^{-3}) \tag{3.28}$$

when (3.26) is the leading approximation. The eigenvalue corresponding to the third mode has also been calculated but is not displayed.

We now argue that the asymptotic expansions (3.27) and (3.28) for Λ are correct for μ both positive and negative although it is clear from (3.25) and (3.26) that, when $\mu > 0$, G_1 has a singularity at a finite value of $\mu^{-\frac{1}{3}}s$. There are two ways of continuing G_1 through this critical layer, either of which justifies (3.27) and (3.28). The first way is to solve the third-order equations obtainable from (3.6) in the region in which

$$s - n\mu^{\frac{1}{3}}/q^{\frac{1}{3}}(q+1)^{\frac{1}{3}} = O(\mu^{-\frac{1}{3}}), \quad K_1 = O(\mu^{\frac{1}{3}}G_1), \tag{3.29}$$

where the viscous terms are important at leading order. This argument has in fact been carried through but is not presented here. Alternatively, analytic continuation of G_1 through the critical layer may be made upon noting that Λ has a small positive imaginary part, so that the singularity is in effect below the real axis of s, with the result that deformation of the contour of integration above the real axis may be made without enclosing between the contour and the axis any singularity of G_1.

Having thus obtained expansions for Λ for both small and large $|\mu|$ it is of interest, before describing the numerical integrations of (3.6) for moderate values of μ, to compare with results obtained from the S-data at large but finite values of R. This will test two of the hypotheses proposed so far: firstly that the near-neutral modes obtained by C.S. are indeed centre modes, i.e. that the scaling (3.1) and transformation (3.2) for ω are appropriate: secondly that the expansions (3.15) for small $|\mu|$ and (3.27) for large $|\mu|$ are being attained.

3.3. *Comparison with the results of C.S. when* $\alpha = n = 1$

As a test of the theory of this section we present in figure 1*a*, *b* the real and imaginary parts ω_r, ω_i of the eigenvalue ω as obtained from the *S*-data at various values of R ranging from 10^4–10^5 with $\alpha = n = 1$. The fact that ω_r, ω_i when multiplied by $R^{\frac{1}{3}}$ and plotted against $(\epsilon - 1)\, R^{\frac{1}{3}}$, respectively lie on smooth curves is indeed consistent with (3.2). The results shown are for the leading mode, i.e. that which is least stable at $\mu = 0$ and subsequently becomes

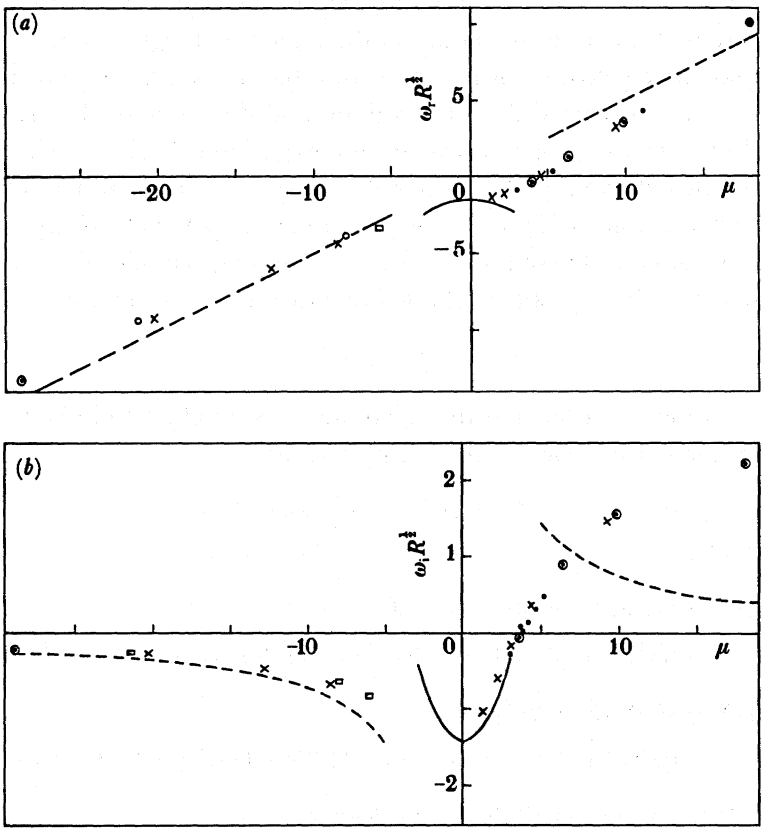

FIGURE 1. (*a*) The real part of $\omega R^{\frac{1}{3}}$ against μ with $n = 1$. Obtained from the *S*-data with $\alpha = 1$ at various values of R: $R = 10^4$, •; $R = 1.3 \times 10^4$, ○; $R = 2.5 \times 10^4$, □; $R = 5 \times 10^4$, ×; $R = 10^5$, ⊙. Asymptotic results from (3.15), ——; and from (3.27), – – –. (*b*) As for (*a*) but the imaginary part of $\omega R^{\frac{1}{3}}$.

unstable as μ increases. Also shown are the asymptotic results for ω obtained above as solutions of the centre-mode equations (3.6). For small $|\mu|$ the formula (3.15) is used, and for large $|\mu|$ we have used (3.27) for μ both positive and negative. We see that for sufficiently small $|\mu|$ the agreement is good, and that for $\mu \ll -1$ it is excellent for both ω_r and ω_i. However for $\mu \gg 1$ the agreement between the *S*-data and the asymptotic expansion (3.27) is poor especially for ω_i, the numerical values of which show no sign of decreasing to zero as predicted by (3.27). In §5 we shall propose a second asymptotic expansion for Λ when $|\mu| \gg 1$, but before so doing we describe the results of the numerical integration of (3.6) at finite values of μ so that we may confirm the accuracy of the *S*-data and examine more closely the status of the expansions introduced in this section.

3.4. *The numerical solution of* (3.6)

Solutions of (3.6) have been obtained for $n = 1, 2, 3$ by two methods. Firstly we tried a finite-element method which, at $\mu = 0$ for example, reproduced well the values of Λ given by (3.11), those for $p \geqslant 1$ occurring in pairs. Also for small $|\mu|$ and for reasonably large negative μ, the curves predicted by the expansions (3.15), (3.20) and (3.27) and (3.28) were being attained. When μ is large and positive the difficulty of the algebraically decaying eigensolutions is exacerbated by the fact that the expected limiting form described in §3.2 has a critical layer. A finite-element mesh was distributed more densely in the anticipated neighbourhood of this layer and the position of the outer boundary of the region of integration was varied. However, it seemed clear that the eigenvalue of the most unstable mode was not deviating far from the predictions of figure 1 constructed from the S-data, and the value of Λ_1 was showing no signs of decreasing in line with the proposed asymptotic expansion (3.27). In view of the difficulty of keeping track by this method of the various modes as μ increases, and as a further test of the S-data against the expansion (3.27), it was decided to develop, for simplicity, a finite-difference approach which (when care is taken to avoid mode jumping) enables the individual modes to be traced as μ increases. The problem of algebraic decay was overcome by setting

$$s^2 = e^{\zeta} - 1 \tag{3.30}$$

in (3.6) and, in addition, in order that the eigenfunctions sought should be bounded and non-zero at the origin, factors s^{n-1} were removed by writing

$$G_1 = s^{n-1}G, \quad K_1 = s^{n-1}K \tag{3.31}$$

so that (3.6) becomes

$$s(\Lambda + s^2)(sK' + nK + nG) + 2n\mu s(sG' + nG)$$
$$= \mathrm{i}[s^2K''' + (3n+1)sK'' + (n-1)(2n+1)K' + nsG'' + n(2n+1)G'], \tag{3.32a}$$

$$s(\Lambda + s^2)(sK' + nG + nK) + 2n^2\mu sG$$
$$= \mathrm{i}[s^2G''' + (3n+1)sG'' + (n-1)(2n+1)G' + nsK'' + n(2n+1)K']. \tag{3.32b}$$

The result of the transformation (3.30) is not shown.

We must now solve (3.32) with G, K regular at the origin and $G, K = O(s^{-2n})$ as $s \to \infty$, with a normalization condition, say $G(0) = 1$. Of chief interest is the form of Λ as a function of μ in particular as $\mu \to \infty$.

The results for $n = 1$ are presented in figure 2*a*, *b* where the real and imaginary parts of Λ are displayed for the five modes that, at $\mu = 0$, are the least stable. Thus at $\mu = 0$ we show the primary mode with $\Lambda = -\sqrt{2}(1+\mathrm{i})$ as given by (3.11) with $p = 0$ and the two pairs $\Lambda = -2e^{\frac{1}{4}i\pi}(2p+1)$ for $p = 1, 2$. Calculations for $\mu \neq 0$ were initiated by using the appropriate formulae (3.15) and (3.20). The eigenvalue crossings at $\mu = 0$ are such that to each coincident eigenvalue there correspond two eigenfunctions.

We first discuss $\mu < 0$ as this, the stable side of the neutral curve, is the simpler. The graph of the eigenvalue of the least stable mode, in the neighbourhood of which, in addition, are shown the results from the S-data displayed also in figure 1, is asymptoting the value obtained from (3.27), and the other two drawn are asymptoting values from (3.28) and the undisplayed result for the third mode respectively. For the leading mode they are graphically

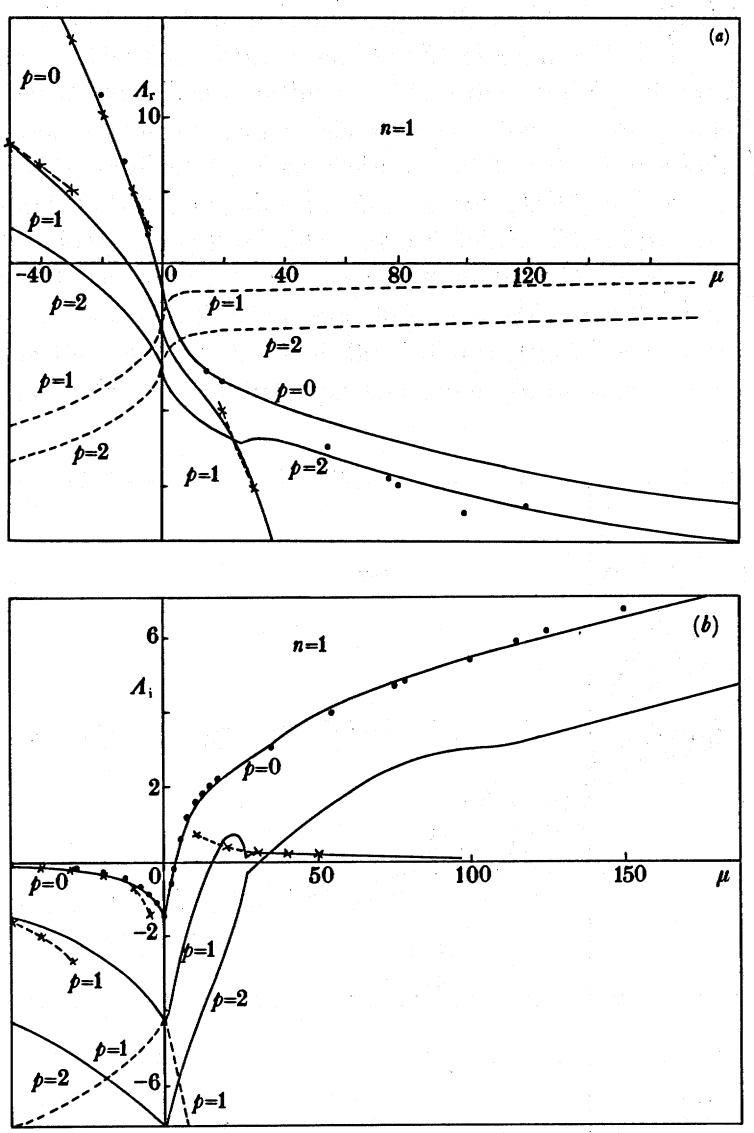

FIGURE 2. (*a*) Real parts of Λ for the leading modes with $n = 1$. Taken from the S-data with $\alpha = 1$, $10^4 \leqslant R \leqslant 10^5$, •. Asymptotic inviscid results from (3.27) and (3.28), --×--. Numerical results for the principal branches distinguished at $\mu = 0$ by $p = 0, 1, 2$ in (3.11), ——; and secondary branches distinguished by $p = 1, 2$, – – –. (*b*) As for (*a*) but the imaginary part of Λ.

indistinguishable by the time μ reaches -10, but we plot the asymptotic form of the second. A comment about the asymptotic form of the increasingly stable modes labelled 'second branch' will be made in §7.

For $\mu > 0$ we show the development of the eigenvalues corresponding to the three modes that are least stable at $\mu = 0$ and subsequently become unstable at μ increases. The leading mode, which is shown together with the results derived from the S-data, becomes neutral at $\mu = \mu_0 \approx 3.8$, but then shows no sign of attaining the asymptotic form (3.27) and neither does the third mode. Both are becoming increasingly unstable. (The fact that the points from the S-data in the graph of Λ_r in figure 2*a* seem to change from the calculated first mode to the third mode as μ increases past 50 is not felt to be significant. Greater accuracy at such large values of

R, Ω could not perhaps be expected from the Galerkin method used there and indeed the deviation is no worse than that in figure 2*b*.) However, the second mode (given by $p = 1$ when $\mu = 0$) does attain the asymptotic limit (3.27). As shown, the curves, particularly that for Λ_1, undergo a rapid change of direction when the eigenvalue becomes almost equal to that for the third ($p = 2$) mode at a value of μ of approximately 25. Such rapid changes of direction at a coincidence, or near coincidence, of eigenvalues leading to unexpected instability, or in this case stability, are not uncommon. Another point of note is that this second mode ($p = 1$) does not attain the same asymptotic form for Λ when $\mu \gg 1$ as it does for $\mu \ll -1$. When $\mu \ll -1$ the value of q in (3.24) is 2 and the corresponding eigenfunction is given by (3.26), though when $\mu \gg 1$ the value of q in (3.24) is unity and the eigenfunction is given by (3.25).

Thus it seems clear that, contrary to our first expectations, Λ is not an analytic function of

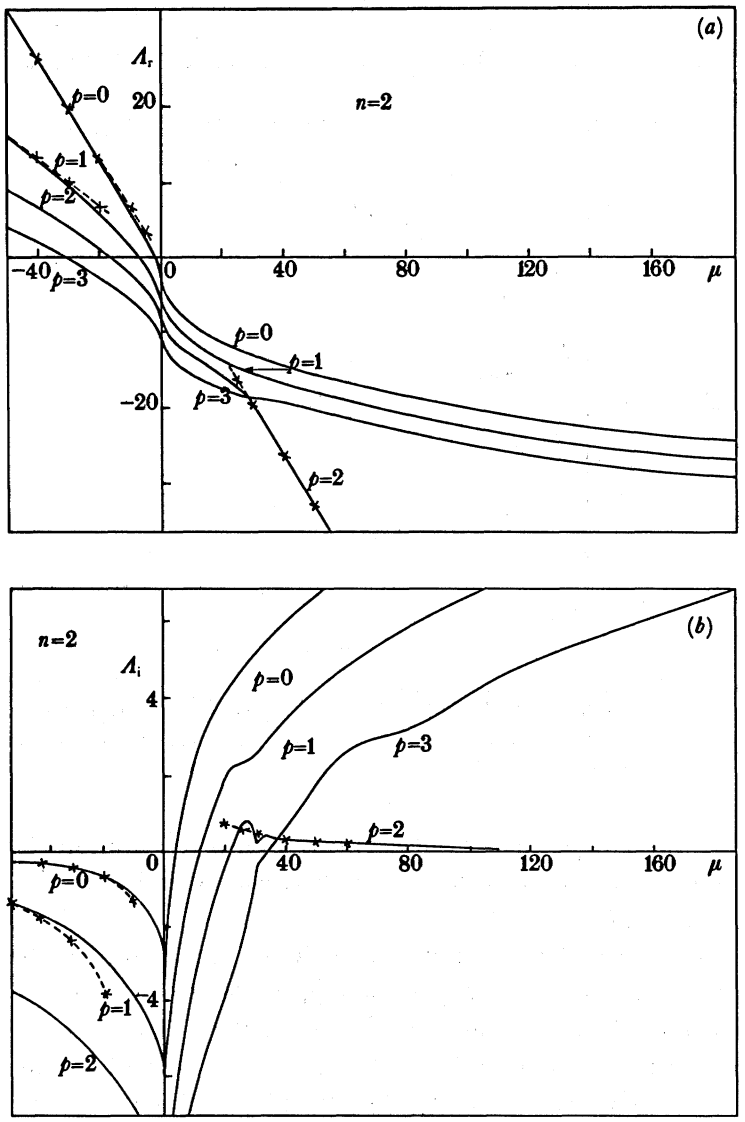

FIGURE 3. (*a*) As for figure 2*a* but $n = 2$, and no results shown from *S*-data. (*b*) As for (*b*) but $n = 2$, and no results shown from *S*-data.

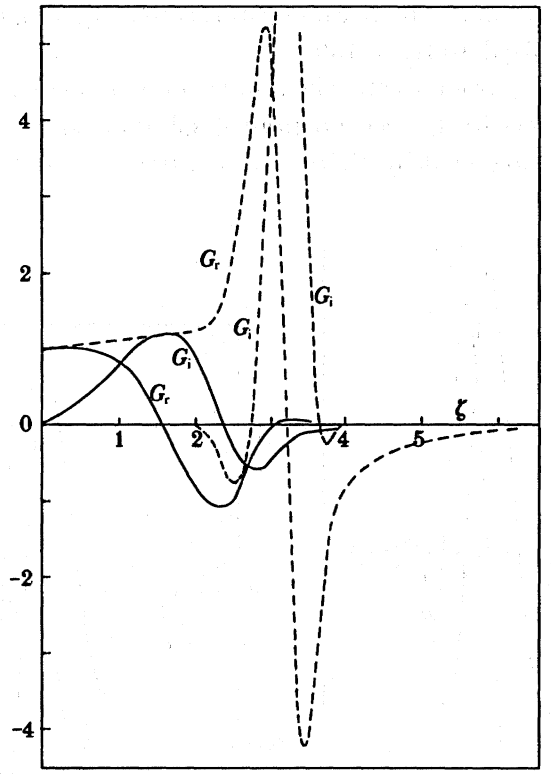

FIGURE 4. Contrast of numerical results for the components of the eigenfunction G at $\mu = 50$ for the viscous leading mode with $n = 1$, ——; (labelled $p = 0$ in figure 2), and the inviscid mode, – – –; (labelled $p = 1$ in figure 2).

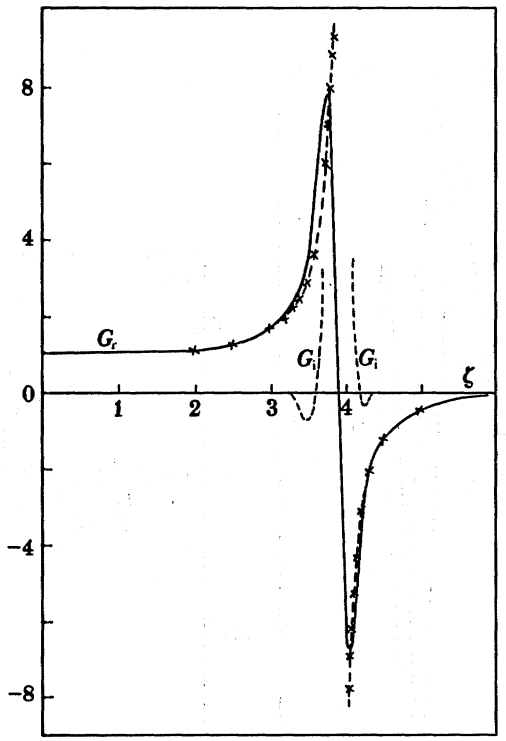

FIGURE 5. Comparison of numerical results (——) for the real part of the eigenfunction G for the inviscid mode with $n = 1$ (labelled $p = 1$ in figure 2) at $\mu = 100$ and the corresponding asymptotic result (3.25), – × – × – ×. The computed imaginary part of G is also shown (– – –).

μ regarded as a complex variable. The reason for this is that the range of s in (3.6) is infinite (see remarks in Drazin & Reid 1981, p. 156).

A similar phenomenon occurs for $n = 2$. The results of the numerical integrations are shown in figure 3a, b though for clarity the second branch solutions are omitted. For small μ the eigenvalue curves are well predicted by (3.15) and (3.20) and for $\mu < 0$ the asymptotic forms

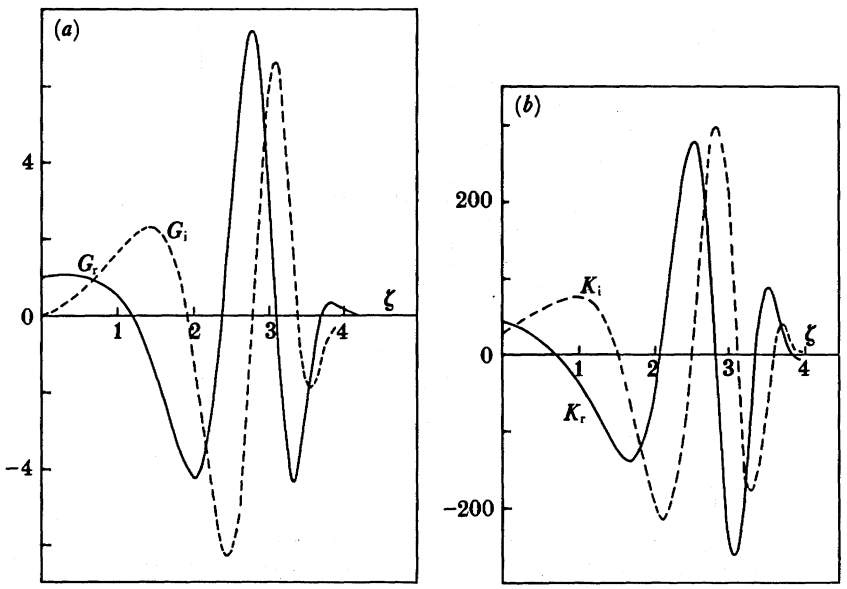

FIGURE 6. (*a*) The real and imaginary part of G for the leading viscous mode with $n = 1$, $\mu = 400$. (*b*) As for (*a*) but eigenfunction K.

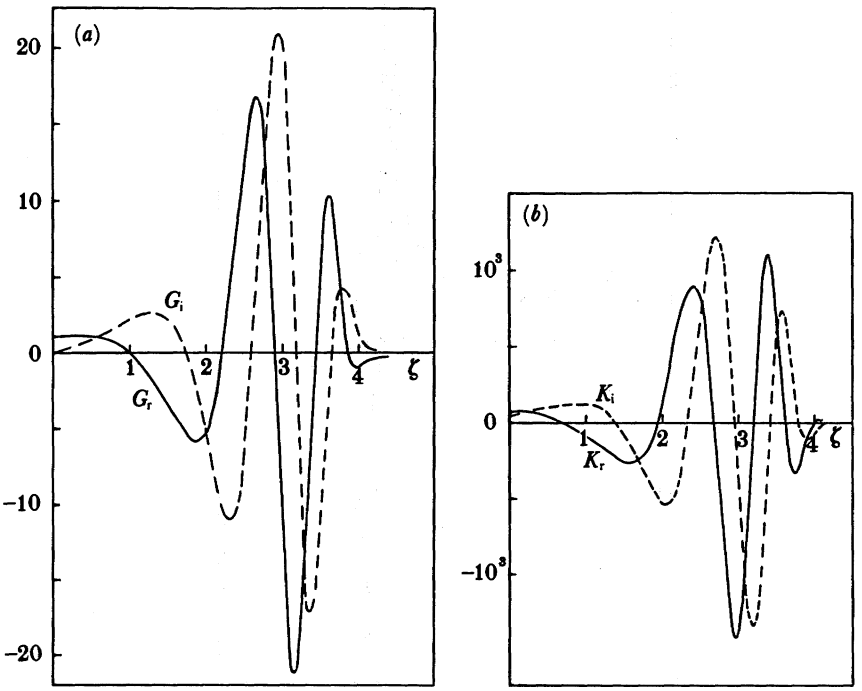

FIGURE 7. (*a*) As for figure 6*a* but $n = 1$, $\mu = 800$. (*b*) As for (*b*) but $n = 1$, $\mu = 800$.

(3.27) and (3.28) are being attained by the two leading modes, and the higher modes are attaining corresponding inviscid limits. However, for $\mu > 0$ it is the third ($p = 2$ at $\mu = 0$) mode that attains the asymptotic form (3.27) after a near coincidence of eigenvalues with the fourth mode. We may also note that when $\mu \gg 1$ the appropriate value of q in (3.24) is 2 although it is 4 when $\mu \ll -1$, and again Λ is not an analytic function of μ.

Before attempting to describe the asymptotic form of those curves that are not attaining the predicted inviscid values (3.27) and (3.28) etc. it is of interest to contrast the eigenfunctions of two modes. We consider $n = 1$ and the two modes of figure 2 that are least stable at $\mu = 0$ ($p = 0, 1$) and then become unstable. In figure 4 we display the real and imaginary parts of the eigenfunctions G for these two modes at $\mu = 50$. The leading $p = 0$ 'viscous' mode has only just begun to take on the oscillatory character that we shall describe below, though the $p = 1$ 'inviscid' mode has already assumed its asymptotic form (3.25). The position of the critical layer is at $s^2 = \frac{1}{2}\mu$ which corresponds to $\zeta = 3.26$ and this is clearly being well produced by the numerical work. In figure 5 we compare the real part of G at $\mu = 100$ for this inviscid mode as given by the numerical integration with its value as predicted by (3.25). The critical layer of thickness $O(\mu^{-\frac{1}{3}})$ is centred at $\zeta = 3.93$; the outer solution for the imaginary part of G is formally smaller but more singular being $O(\mu^{-2}|1 - 2s^2\mu^{-1}|^{-4})$ as $s^2 \to \frac{1}{2}\mu$.

As μ increases the leading viscous eigensolution gradually becomes more oscillatory with oscillations of increasing amplitude. The region of oscillation slowly moves to larger values of s and spreads out in a manner quite unlike the concentration in the neighbourhood of the critical layer of the perturbation associated with the inviscid mode. In §5 we argue that this oscillation extends throughout a region in which $s = O(\mu^{\frac{1}{3}})$ with $K = O(\mu^{\frac{2}{3}}G)$ and that the amplitudes of the oscillations are exponentially large, specifically $O(\exp \mu^{\frac{1}{3}})$. These trends are exhibited in figures 6 and 7, which show the eigenfunctions at $\mu = 400$ and 800. Figures 8 and 9

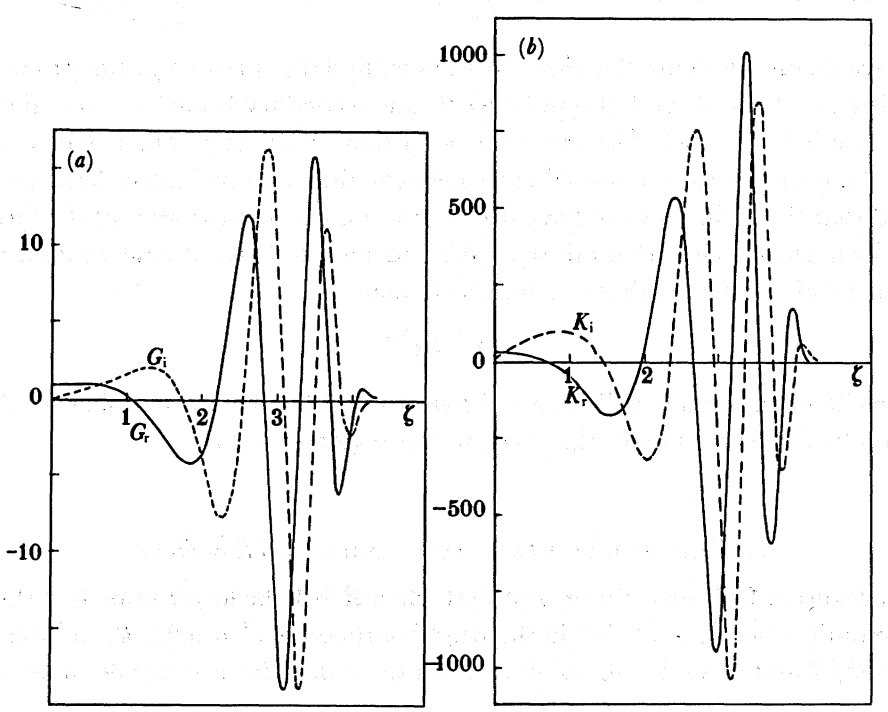

FIGURE 8. (*a*) As for figure 6*a* but $n = 2$, $\mu = 400$. (*b*) As for (*b*) but $n = 2$, $\mu = 400$.

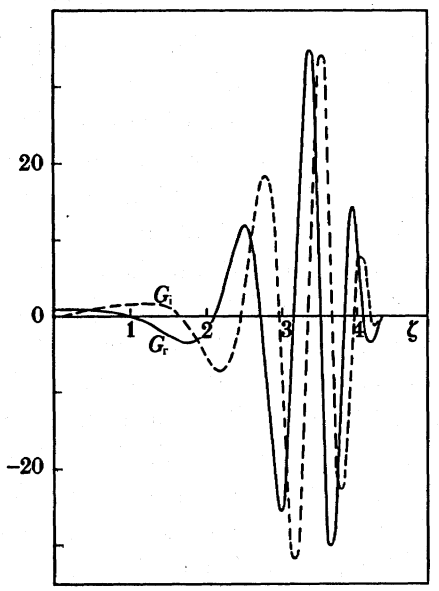

FIGURE 9. As for figure 6*a* but $n = 3$, $\mu = 400$.

show the effect of increasing n for fixed μ. The effect is similar to that of increasing μ for fixed n. Solutions were computed for values of μ up to 1000 and although the eigenvalues are expected to be reasonably accurate (say to three significant figures) at these values the eigenfunctions themselves begin to lose precise definition, though where necessary the outer boundary was taken at $\zeta = 12$ ($s = 403$) and the number of points across the region to be 1200. The effect of varying both these quantities was considered. We conjecture that the final algebraic decay for these highly oscillatory solutions takes place with $s = O(\mu^{\frac{1}{3}})$ and support this by the analysis of §5.

A distinctive feature of figure 2 is that, for sufficiently large positive μ, the primary branch curves labelled $p = 0$ and 2 (and also in figure 2*a* the secondary branch curves labelled $p = 1$ and 2) are essentially parallel. The same is true of those labelled $p = 0$, 1 and 3 in figure 3. The form of these curves was monitored extremely carefully as μ increased, because initially it was expected that these curves would eventually take on the inviscid asymptotic form of §3.2. However, it soon became clear that this is not the outcome, and an estimate from the numerical results for the leading mode with $n = 1$ indicated that

$$\mu^{-\frac{1}{3}}\Lambda \to 3\,\mathrm{e}^{\frac{4}{3}\mathrm{i}\pi} \tag{3.33}$$

as $\mu \to \infty$. Justification for this will be put forward in §5 but before so doing we discuss the analogous results for centre modes that exist in the region $\epsilon^2 \approx R$.

4. The modal structure when $\epsilon^2/R = O(1)$

The calculations of C.S. strongly suggest that when $R \gg 1$ the lower branch of their neutral curve for the most unstable mode lies in the neighbourhood of $\epsilon^2 = 0.023R$. In table 1 we give the values of ϵ^2/R and of $\epsilon - 1 - \omega_r$ obtained from the S-data for a range of values of R when $\alpha = n = 1$.

We now show that, when $\epsilon^2 = O(R)$ and $R \gg 1$, there is a class of eigenfunctions, again centre

TABLE 1. NEUTRAL CONDITIONS AT VARIOUS VALUES OF R FROM THE S-DATA

R	ϵ^2/R	$\epsilon-1-\omega_r$
10000	0.0219	0.859
21000	0.0226	0.874
40000	0.0231	0.884
60000	0.0233	0.889
100000	0.0235	0.893

modes as in the neighbourhood of the upper branch when $\epsilon n \approx \alpha$, whose properties are dependent on $\alpha\epsilon^2/R$ and n only, and are independent of R and α.

To obtain these centre-mode equations we write in (2.2)

$$\left.\begin{aligned} \bar{F} &= \alpha^{-\frac{3}{4}}R^{\frac{1}{4}}\bar{f}_1(s), \quad \bar{G} = \bar{g}_1(s), \\ \bar{H} &= \bar{h}_1(s), \quad \bar{P} = (\alpha R)^{-\frac{1}{4}}(\sigma n)^{-1}\bar{p}_1(s), \end{aligned}\right\} \tag{4.1}$$

where σ is defined as

$$\sigma = (\alpha R)^{\frac{1}{2}}(\epsilon n\alpha)^{-1} \tag{4.2}$$

and $r = (\alpha R)^{-\frac{1}{4}}s$ again as in (3.1). We set

$$\omega = \alpha\epsilon - n + \lambda(n\sigma)^{-1}, \tag{4.3}$$

where λ has to be found as a function of σ, n. Then

$$\gamma = -(1/n\sigma)(\lambda + s^2), \tag{4.4}$$

and by direct substitution into (2.2)

$$s\bar{f}_1 + s\bar{g}_1' + \bar{g}_1 - n\bar{h}_1 = 0, \tag{4.5a}$$

$$(\lambda+s^2)\bar{f}_1 + 2s\bar{g}_1 = \mathrm{i}\left[\bar{f}_1'' + \frac{1}{s}\bar{f}_1' - \frac{n^2}{s^2}\bar{f}_1\right], \tag{4.5b}$$

$$(\lambda+s^2)\bar{g}_1 - 2n\sigma\bar{h}_1 + \bar{p}_1' = \mathrm{i}\left[\bar{g}_1'' + \frac{1}{s}\bar{g}_1' - \frac{n^2+1}{s^2}\bar{g}_1 + \frac{2n\bar{h}_1}{s^2}\right], \tag{4.5c}$$

$$(\lambda+s^2)\bar{h}_1 - 2n\sigma\bar{g}_1 + n\bar{p}_1/s = \mathrm{i}\left[\bar{h}_1'' + \frac{1}{s}\bar{h}_1' - \frac{n^2+1}{s^2}\bar{h}_1 + \frac{2n\bar{g}_1}{s^2}\right] \tag{4.5d}$$

provided that terms that are of relative order $R^{-\frac{1}{4}}$ are uniformly neglected. For an acceptable solution of (4.5) we require $\bar{f}_1, \bar{g}_1, \bar{h}_1$ to be regular at $s = 0$ and to vanish as $s \to \infty$ for consistency with the assumption that the disturbance is concentrated near the axis of the pipe. These centre-mode equations have also been obtained by Berry & Norbury (1985) and solved, with $n = 1$, for the value of σ corresponding to neutral stability. They obtained $\sigma = 6.5$ or $\alpha\epsilon^2/R = 0.024$ in good agreement with the results of table 1; the corresponding value of λ is 5.8. We extend their work and consider the solutions of (4.5) for all values of σ.

As will be clear from the numerical solutions of §4.2 the system (4.5) has no real values of σ where the eigenvalues are equal in pairs as was the situation in §3.1 at $\mu = 0$. Thus it is unlikely that eigenmodes will be easy to find analytically in this case, though the fact that solutions exist for finite complex σ may be established. A simple family is given by

$$\bar{g}_1 = \bar{h}_1 = \mathrm{e}^{-\frac{1}{2}\beta s^2}, \quad \bar{f}_1 = s\beta\,\mathrm{e}^{-\frac{1}{2}\beta s^2}, \quad \bar{p}_1 = 0 \tag{4.6}$$

with $\beta = e^{-\frac{1}{4}i\pi}$, which satisfies (4.5) provided $n = 1$ and $\sigma = -2/\beta$, $\lambda = -6/\beta$, though as we shall see, in general the decay is algebraic $O(s^{-1-\sqrt{(n^2+4)}})$ for $\bar{g}_1$, rather than exponential as in (4.6).

As was the case with (3.6) we shall find that the solutions of (4.5) have two possible limiting forms when $\sigma \gg 1$. Again, one is inviscid and is the analogue of the solutions presented in §3.2.

4.1. *The inviscid limit when* $\sigma \gg 1$

When $\sigma \gg 1$ it is possible to write down an inviscid limit of equations (4.5) in which $s = O(\sigma^{\frac{1}{2}})$ and the right-hand sides are, on the assumption that $\lambda = O(\sigma)$, of relative order $O(\sigma^{-2})$. By elimination we obtain for $\bar{g}_1$ the equation

$$s^2\bar{g}_1'' + 3s\bar{g}_1' + \left[1 - n^2 - \frac{4s^2}{\lambda + s^2} - \frac{4n^2\sigma s^2}{(\lambda + s^2)^2}\right]\bar{g}_1 = 0, \tag{4.7}$$

an equation similar in form to (3.22). The solution of (4.7) regular at $s = 0$ is

$$\bar{g}_1(s) = \frac{s^{n-1}}{(\lambda + s^2)^k} F\left(a_1, b_1, n+1, -\frac{s^2}{\lambda}\right), \tag{4.8}$$

where

$$a_1 = \tfrac{1}{2}n - k - \tfrac{1}{2}(n^2+4)^{\frac{1}{2}}, \quad b_1 = \tfrac{1}{2}n - k + \tfrac{1}{2}(n^2+4)^{\frac{1}{2}} \tag{4.9}$$

if k is defined by

$$n^2\sigma/\lambda = -k(k+1). \tag{4.10}$$

So that $\bar{g}_1$ may decay as $s \to \infty$ it is necessary to choose b_1 to be a negative integer or zero so that the hypergeometric function F reduces to a polynomial. This leads to a sequence of values for k and hence, by (4.10), to a sequence of values of σ. If we take as principal eigensolution that given by (4.8) with the weakest singularity, then this is

$$\bar{g}_1(s) = s^{n-1}/(\lambda + s^2)^k \tag{4.11}$$

with

$$k = \tfrac{1}{2}n + \tfrac{1}{2}(n^2+4)^{\frac{1}{2}}, \quad \lambda = -\frac{4n^2\sigma}{[n + (n^2+4)^{\frac{1}{2}}]\,[n+2+(n^2+4)^{\frac{1}{2}}]}. \tag{4.12}$$

Hence from (4.3), as $\sigma \to \infty$,

$$\omega \to \alpha\epsilon - n - \frac{4n}{[n + (n^2+4)^{\frac{1}{2}}]\,[n+2+(n^2+4)^{\frac{1}{2}}]}. \tag{4.13}$$

The presence of the singularity at $s = (-\lambda)^{\frac{1}{2}}$ at first sight seems to raise difficulties about the validity of the neglect of the viscous terms. We may however justify it on similar grounds to those described in §3.2. A first-order correction to (4.13) may be obtained by substituting (4.11) and (4.12) into the right-hand sides of (4.5) and expanding λ in descending powers of σ^2. The condition that the correction satisfies the boundary conditions then leads to the result

$$\omega_1 = \frac{2(n+1)\,(k+1)^3\,(2k-n+1)}{n(2k+3)\,\sigma^2}, \tag{4.14}$$

which is to be multiplied by i and added to (4.13) which is then in error by $O(\sigma^{-4})$.

As in §3 there are two questions to be answered. The first is whether the centre-mode

equations (4.5) are the correct limits of the full equations as $R \to \infty$, $\epsilon \to \infty$ with $\epsilon^2/R = O(1)$. Secondly, as $\sigma \to \infty$ in (4.5) is the inviscid limit (4.11) and (4.13) attained or is the limiting solution of an entirely different form? Comparison with results for the primary mode with $\alpha = n = 1$ extracted from the S-data at various values of R confirms that $\epsilon - 1 - \omega_r$ and ω_i are functions of $\epsilon/R^{\frac{1}{3}}$ for sufficiently large ϵ and R. However, again, as in §3.3, the asymptotic forms (4.11) and (4.13) do not seem to be being attained by the S-data.

To resolve this it is necessary to find numerical solutions of (4.5) at finite values of σ and we now describe such solutions below.

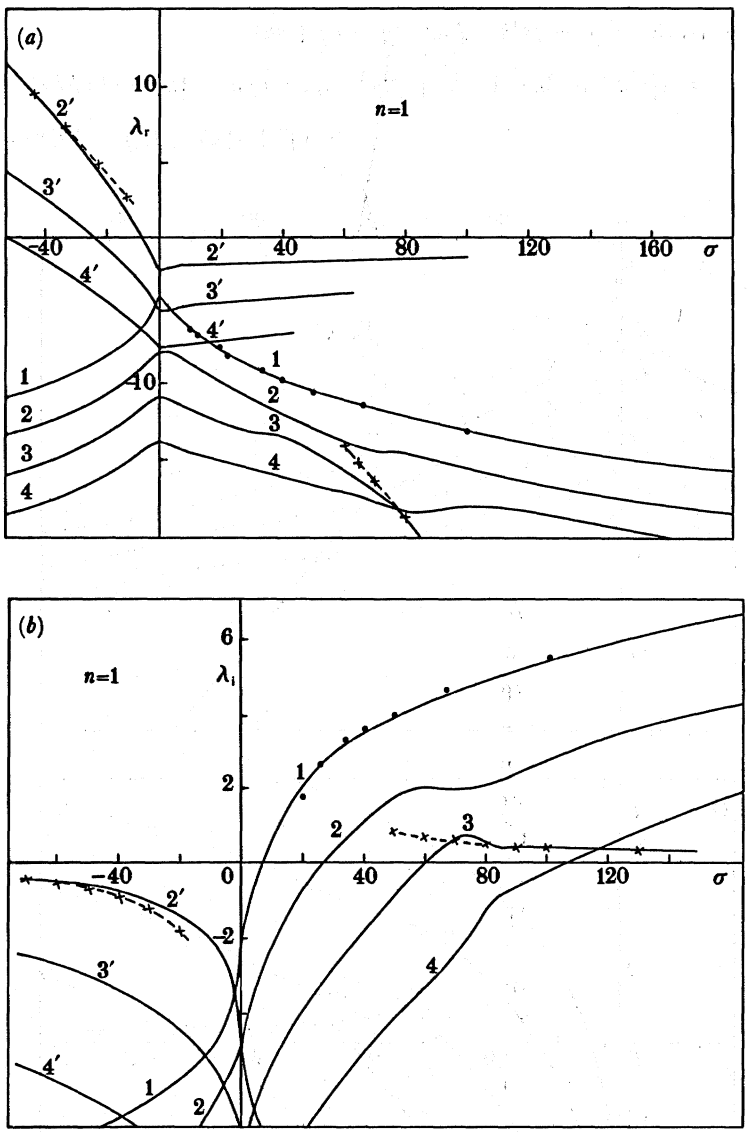

FIGURE 10. (*a*) Real parts of λ for the leading modes with $n = 1$. Taken from the S-data with $\alpha = 1$, $10^4 \leqslant R \leqslant 10^5$, ●. Present numerical results, ——. Asymptotic inviscid results from (4.13) and (4.14), – – × – –. (*b*) As for (*a*) but the imaginary parts of λ.

4.2. *The numerical solution of* (4.5)

Solutions of (4.5) were sought after elimination in favour of $\bar{g}_1$, $\bar{h}_1$ and substitution of

$$\bar{g}_1 = s^{n-1}g, \quad \bar{h}_1 = -s^{n-1}h \tag{4.15}$$

so that they become

$$(\lambda+s^2)(s^2g'+nsg+nsh)-2s^3g$$
$$= [s^2g'''+(3n-1)sg''+(2n^2-5n+1)g'-4n(n-1)g/s$$
$$+nsh''+n(2n-3)h'-4n(n-1)h/s], \tag{4.16a}$$

$$(\lambda+s^2)(s^2h'+nsh+nsg)+2s^3h+2n\sigma s(sg'+ng+nh)$$
$$= \mathrm{i}[s^2h'''+(3n-1)sh''+(2n^2-5n+1)h'-4n(n-1)h/s$$
$$+nsg''+n(2n-3)g'-4n(n-1)g/s], \tag{4.16b}$$

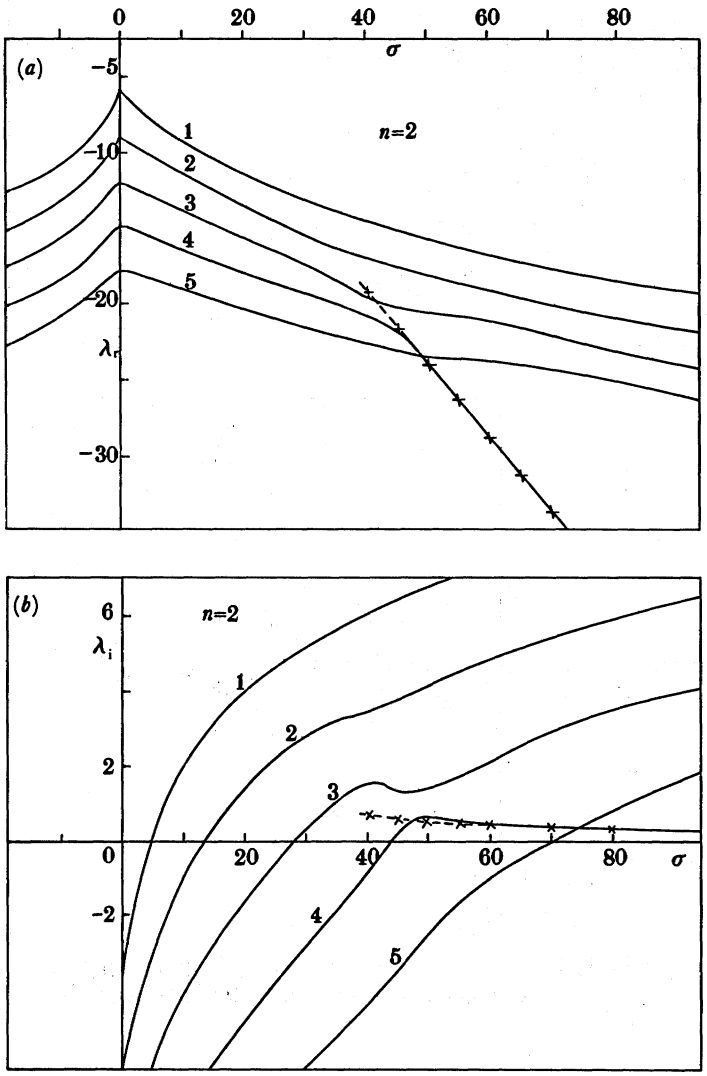

FIGURE 11. (*a*) As for figure 10*a* but $n = 2$, and no results shown from *S*-data. (*b*) As for (*b*) but $n = 2$, and no results shown from *S*-data.

which must be solved with g and h regular at the origin, $g(0) = 1$ and $g, h = O(s^{-n-(n^2+4)^{\frac{1}{2}}})$ as $s \to \infty$. Again, to eliminate this algebraic decay, the transformation $s^2 = e^{\zeta} - 1$ was made as in (3.30).

To solve (4.16) the finite-difference method of §3.3 was used. In figure 10 we display, for $n = 1$, the real and imaginary parts of λ as a function of σ for the modes that are least stable at $\sigma = 0$. The value of σ, $\sigma = 6.45$, at which the first mode becomes neutral is in agreement with $\sigma = 6.5$ given by Berry & Norbury (1985). Also shown on this figure are results derived from the leading mode of the S-data with $\alpha = n = 1$. These are seen to lie well on the curve labelled 1. In figure 11 we undertake the same task for $n = 2$, though we omit the eigenvalues of those modes that immediately become increasingly stable as σ increases from zero. Although σ as defined in (4.2) is positive, negative values of σ are included for completeness and for comparison with the results of §3 for the centre modes where $\epsilon n \approx \alpha$; the curves shown for $\sigma < 0$ in fact correspond to stable solutions for *negative* axial wavenumber α. For small σ the figures look somewhat similar to figures 2 and 3 but we do not have the simplification of pairing of eigenvalues and analytically realisable eigenfunctions. When σ is large and negative the curves labelled 2′, 3′ and 4′ attain the asymptotic forms given by (4.10) with k as in (4.9) and $b_1 = 0, -1, -2$, respectively. The eigenfunction is obtained from (4.11) and for 2′ the value of λ_1 follows from (4.14). The probable asymptotic form of those labelled 1, 2, 3 and 4 is noted in §7.

As in the centre-mode problem of §3, neither when $n = 1$ or $n = 2$ does the leading eigenmode (labelled 1) attain the inviscid asymptotic form given by (4.10) and (4.11). This asymptotic form is attained by the third mode when $n = 1$ and the fourth when $n = 2$. As an illustration of the attainment of this inviscid limit we plot, in figure 12, the third mode with $n = 1$ and

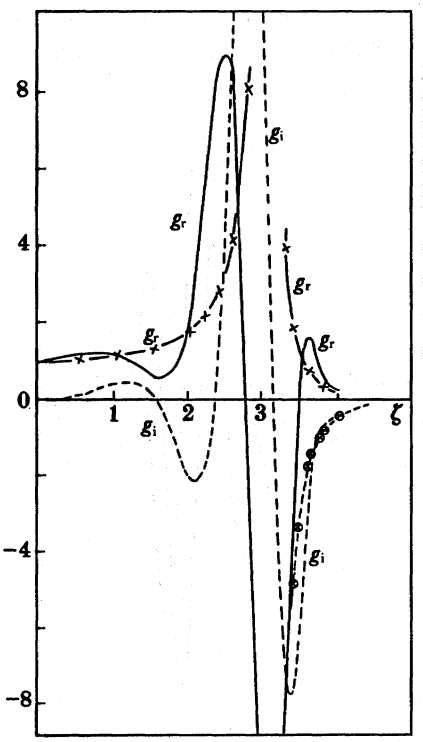

FIGURE 12. Comparisons of numerical results (——, – – –), for g_r and g_i with $n = 1$ at $\sigma = 90$ and the asymptotic results (–×–, –⊗–) from (4.11).

$\sigma = 90$. The critical layer at $s^2 = \sigma/k(k+1)$ is at $\zeta = 3.10$, and we also plot $g(s) = (\lambda + s^2)^{-k}$ as from (4.11). This means that for $\zeta < 3.10$, the asymptotic form of g is real to leading order, but for $\zeta > 3.10$, this asymptotic form has both a real and an imaginary part because the factor $|\sigma/k(k+1) - s^2|^k$ is multiplied by $e^{-i\pi k}$ as s^2 increases through $\sigma/k(k+1)$. For $\zeta < 3.10$, the imaginary part of g is more singular though formally smaller, namely $O(\sigma^{-2}|1-k(k+1)\, s^2\sigma^{-1}|^{-k-3})$.

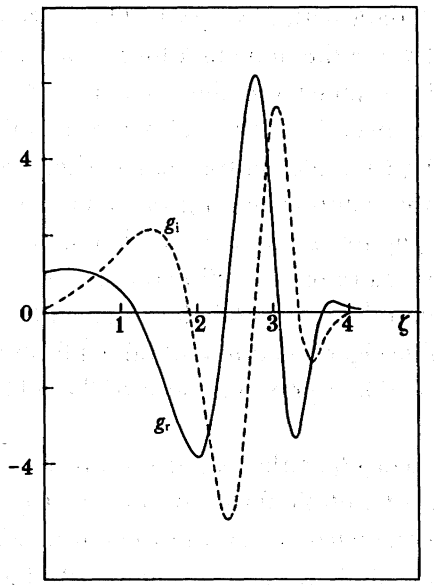

FIGURE 13. The leading viscous mode for $n = 1$, $\sigma = 400$.

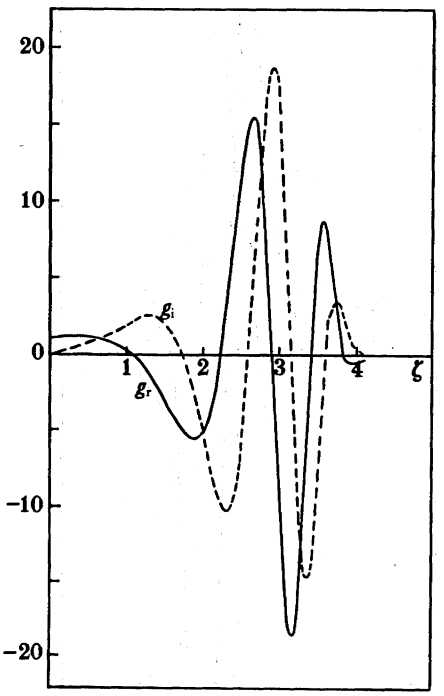

FIGURE 14. The leading viscous mode for $n = 1$, $\sigma = 800$.

PHILOSOPHICAL TRANSACTIONS OF THE ROYAL SOCIETY A MATHEMATICAL, PHYSICAL & ENGINEERING SCIENCES

In trials to ascertain the asymptotic form of the leading mode values of σ up to 1000 were considered. However, it emerged that on and after $\sigma \approx 100$ the results for λ as a function of σ were graphically indistinguishable from those of the problem of §3 for Λ as a function of μ. Once this was suspected great care was exercised to confirm the conjecture, and comparison of figures 13, 14 and 15 with figures 6*a*, 7*a* and 8*a*, respectively, reveals the similarity of g and G as functions of ζ at $\sigma = \mu = 400$ and $\sigma = \mu = 800$. In §6 we show that the proposed asymptotic forms are, to leading order, indeed the same except at very large values of s, specifically when $s = O(\mu^{\frac{1}{3}})$ or $s = O(\sigma^{\frac{1}{3}})$, where the algebraic decays for G and g differ.

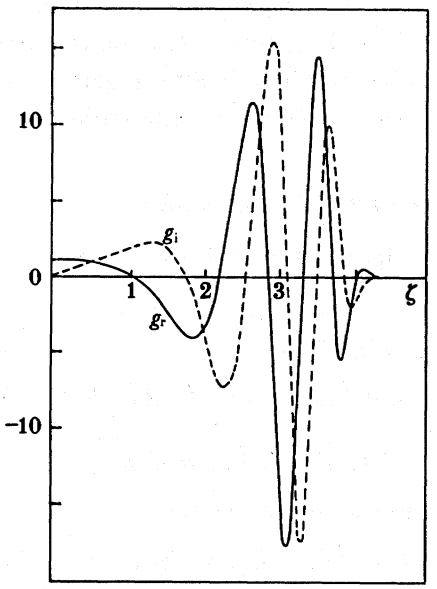

FIGURE 15. The leading viscous mode for $n = 2$, $\sigma = 400$.

As a final comment in this section we note that, as was the case with Λ and μ, the eigenvalue λ is not an analytic function of σ. For example, with $n = 1$, the third mode takes the inviscid form (4.10) with $b_1 = 0$ in (4.9) when $\sigma \gg 1$, but when $\sigma \ll -1$ the curves marked 1 in figures 10 and 11 are not assuming an inviscid limit, though an inviscid limit is being attained by those marked 2′, 3′ and 4′. Again as was the situation with figures 2 and 3 we note how parallel the curves of figures 10 and 11 which do not correspond to the inviscid limit become and, in the following section, analyse the form of these 'viscous' modes.

5. THE HIGHLY OSCILLATORY VISCOUS EIGENSOLUTIONS AT LARGE VALUES OF μ AND σ

In this section we attempt to analyse the forms of the highly oscillatory solutions of (3.32) and (4.16) as the parameters μ and σ increase, and to justify the formula (3.33) conjectured from the numerical work; the same formula will be shown to hold for the most unstable mode of (4.16), also when $n = 1$, with μ replaced by σ and Λ by λ. To do this we concentrate on (3.32) and then show that, except in the very outer region where the algebraic decays differ, the systems (3.32) and (4.16) are identical to leading order. This means that these solutions

hold, at sufficiently large values of R, from one branch of the neutral curve to the other, i.e. right across the unstable region in the (R, Ω)-plane.

It emerges that, to discuss these viscous eigensolutions, it is necessary to divide the range of s into four regions, namely $s = O(\mu^{-\frac{1}{6}})$, $s = O(1)$, $s = O(\mu^{\frac{1}{3}})$ and $s = O(\mu^{\frac{1}{2}})$. In the first the solutions are Bessel functions but not of real argument and therefore, because they are regular at the origin, they are exponentially large at the outer edge. The second serves to distinguish the eigenvalues of the various modes whose asymptotic form for the modes of this type is the same for each to leading order. In the third region the W.K.B. approximation is appropriate and in the fourth the final algebraic decay takes place.

We first present the solutions in the four regions for the system (3.32) and then show how the matching determines the eigenvalues. It emerges that the required formulae are available at an earlier stage of the expansion if we consider (3.32b) together with the equation obtained by eliminating μ between (3.32a) and (3.32b) by differentiation and subtraction. This new equation is

$$s^2(\Lambda+s^2)(sG''+(2n+1)G')+2s^3(sG'+nG+nK)$$
$$=\mathrm{i}[s^3G^{\mathrm{iv}}+(4n+2)s^2G'''+(4n^2-1)sG''-(4n^2-1)G'], \quad (5.1a)$$

and (3.32b) is

$$s(\Lambda+s^2)(sG'+nG+nK)+2n^2\mu sG$$
$$=\mathrm{i}[s^2G'''+(3n+1)sG''+(n-1)(2n+1)G'+nsK''+n(2n+1)K']. \quad (5.1b)$$

5.1. *Region* 1: $s = O(\mu^{-\frac{1}{6}})$

In this region, which extends to the origin, we set

$$s=\mu^{-\frac{1}{6}}t, \quad \Lambda=\mu^{\frac{1}{3}}\Gamma, \quad G(s)=\tilde{G}(t), \quad K(s)=\mu^{\frac{2}{3}}\tilde{K}(t) \quad (5.2)$$

in (5.1) and retain the leading-order terms only. This results in, from (5.1b),

$$\Gamma t\tilde{K}+2nt\tilde{G}=\mathrm{i}[t\tilde{K}''+(2n+1)\tilde{K}') \quad (5.3a)$$

and, from (5.1a),

$$\Gamma t^2[t\tilde{G}''+(2n+1)\tilde{G}']+2nt^3\tilde{K}=\mathrm{i}[t^3\tilde{G}^{\mathrm{iv}}+(4n+2)t^2\tilde{G}'''+(4n^2-1)t\tilde{G}''-(4n^2-1)\tilde{G}']. \quad (5.3b)$$

Now (5.3) are the same equations as were solved by Pedley (1969) in his small axial wavenumber solution of this problem, though we shall not here be seeking a solution that vanishes at a finite value of the independent variable as in his case. However, either by the method he employed, or by direct substitution, we may show that the solution regular at the origin is

$$\tilde{G}=\sum_{j=1}^{3}A_j\frac{J_n(p_jt)}{(p_jt)^n}, \quad \tilde{K}=\sum_{j=1}^{3}\mathrm{i}A_jp_j\frac{J_n(p_jt)}{(p_jt)^n}, \quad (5.4)$$

where the A_j are constants, J_n is a Bessel function of the first kind and p_j satisfies the cubic

$$\tilde{p}(\tilde{p}^2-\mathrm{i}\Gamma)=2n. \quad (5.5)$$

If, as we shall assume below and argue that it is correct, two of the $\tilde{p}$ are equal the missing solution is

$$\tilde{G}=\frac{J_n'(\tilde{p}t)}{(\tilde{p}t)^{n-1}}, \quad \tilde{K}=\mathrm{i}\tilde{p}\left\{\frac{J_n(\tilde{p}t)}{(\tilde{p}t)^n}+\frac{J_n'(\tilde{p}t)}{(\tilde{p}t)^{n-1}}\right\}. \quad (5.6)$$

As t increases along the real axis, $\tilde{G}$ will become exponentially large unless p_j is real as it was in Pedley's situation. If p_j is real then $\tilde{G}$, $\tilde{K}$ in (5.4) decay as $s^{-n-\frac{1}{2}}$ as $s\to\infty$ whereas the decay for (3.32) is s^{-2n}. Thus the outer boundary condition is not satisfied in this region $t=O(1)$. Because the numerical work indicates that $\tilde{p}$ is not real we are prepared to accept that $\tilde{G}$ is exponentially large. We shall present an argument that matches both the exponentially large and the exponentially small terms in $\tilde{G}$ which turns out to be possible only if $\tilde{p}$ in (5.5) has equal roots. There are three possible values of Γ for $\tilde{p}$ to have equal roots, i.e.

$$\Gamma = 3n^{\frac{2}{3}}\mathrm{e}^{\frac{5}{6}\mathrm{i}\pi} \quad \text{with} \quad p_1 = p_2 = n^{\frac{1}{3}}\mathrm{e}^{-\frac{1}{3}\mathrm{i}\pi}, \tag{5.7a}$$

$$\Gamma = 3n^{\frac{2}{3}}\mathrm{e}^{\frac{1}{6}\mathrm{i}\pi} \quad \text{with} \quad p_1 = p_2 = n^{\frac{1}{3}}\mathrm{e}^{\frac{1}{3}\mathrm{i}\pi}, \tag{5.7b}$$

$$\Gamma = -3n^{\frac{2}{3}}\mathrm{i} \quad \text{with} \quad p_1 = p_2 = -n^{\frac{1}{3}}, \tag{5.7c}$$

and $p_3 = -2p_1$ in each case. The first of these agrees with the prediction (3.33) from the numerical work. It corresponds, for $\mu>0$, to an unstable mode with $\Gamma_{\mathrm{i}}>0$, $\Gamma_{\mathrm{r}}<0$, and evidence will be put forward below that it is applicable to the curves labelled $p=0$, 2 in figures 2 and $p=0$, 1, 3 in figures 3. The value of Γ in (5.7b) also corresponds to an unstable mode but with $\Gamma_{\mathrm{r}}>0$ and we did not encounter this. The third value of Γ, (5.7c), a stable mode, with $\Gamma_{\mathrm{r}}=0$ to leading order, is most likely to correspond to those labelled 'second branch' in figure 2. If $\mu<0$, because of the factor $\mu^{\frac{1}{3}}$ in (5.2), then (5.7a) and (5.7b) correspond to stable modes whereas (5.7c) is unstable. Because $\mu<0$ is the stable side of the neutral curve we naturally did not encounter (5.7c) but the second branch curves in figure 2 are in reasonable agreement with (5.7b) on changing the sign of μ in (5.2).

We now proceed on the assumption that for the unstable modes with $\mu\gg 1$ the value of Γ is given to leading order by (5.7a) and demonstrate that the suggested matching indeed requires equal roots for $\tilde{p}$. We consider the matching for $\tilde{G}$ only, as it follows from (5.3b) that $\tilde{K}$ is then automatic. The asymptotic expansion of (5.4) for $|t|\gg 1$ is now required with p_1 defined in (5.7a) and

$$\tilde{G} = A_1\frac{J_n(p_1t)}{(p_1t)^n} + A_2\frac{J_n'(p_1t)}{(p_1t)^{n-1}} + A_3\frac{J_n(2p_1t)}{(p_1t)^n}, \tag{5.8}$$

and because p_1 is complex the exponentially small terms in these expansions are, in the sense of Poincare, indeterminate if t is large and real. As we wish to match such terms we change the direction of the path of integration so that it makes an angle of $\frac{1}{3}\pi$ with the positive real t-axis. This will change the eigenfunction, but leave the eigenvalue unaltered as long as the final part of the path in the s-plane is along the positive real axis and no singularity of the equation is enclosed between the displaced path and the real axis of s. Because p_1t ($\equiv t_1$) is now real it follows from (5.8) that, for $|t|\gg 1$,

$$\tilde{G}\approx(2\pi)^{-\frac{1}{2}}t_1^{-n-\frac{1}{2}}\{A_2\,\mathrm{i}t_1(\mathrm{e}^{\mathrm{i}\chi}-\mathrm{e}^{-\mathrm{i}\chi}) + (A_1-\tfrac{1}{8}(4n^2+3)\,A_2)\,(\mathrm{e}^{\mathrm{i}\chi}+\mathrm{e}^{-\mathrm{i}\chi}) + (A_3/\sqrt{2})\,(\mathrm{e}^{\mathrm{i}\chi_3}+\mathrm{e}^{-\mathrm{i}\chi_3})\}, \tag{5.9}$$

where terms $O(t_1^{-n-\frac{3}{2}})$ have been omitted and

$$\chi = t_1-\tfrac{1}{2}n\pi-\tfrac{3}{4}\pi, \quad \chi_3 = 2t_1-\tfrac{1}{2}n\pi-\tfrac{3}{4}\pi. \tag{5.10}$$

Before further considering (5.9) we present the solution at the very outer edge of the layer where the algebraic decay takes place.

5.2. *Region* 4: *the very outer solution,* $s = O(\mu^{\frac{1}{2}})$

This is the region in which the correct algebraic decay, $G = O(s^{-2n})$ in (3.32) and $g = O(s^{-n-(n^2+4)^{\frac{1}{2}}})$ in (4.16), takes place. It is the only region in which the limiting form of these viscous eigensolutions for the two systems differs to leading order in σ or μ. The solution is inviscid in each case and satisfies the left-hand sides of (5.1) and (4.16) respectively. From (5.1) we find that the algebraically decaying solution in the region where $s = O(\mu^{\frac{1}{4}})$ is

$$G = r_1^{-n} J_n(2ni/r_1), \quad s = \mu^{\frac{1}{2}} r_1. \tag{5.11}$$

For (4.16) the corresponding solution in the region $s = O(\sigma^{\frac{1}{2}})$ is

$$g = r_1^{-n} J_{(n^2+4)^{\frac{1}{2}}}(2ni/r_1), \quad s = \sigma^{\frac{1}{2}} r_1. \tag{5.12}$$

To determine the eigenvalues we are going to require the match of both exponentials so, to determine the term that would be exponentially small when r_1 is real and small, we let r_1 tend to zero along a path with $\arg r_1 = -\frac{1}{2}\pi$. Thus

$$G \approx E r_1^{-n+\frac{1}{2}} \left\{ \exp\left[\mathrm{i}\left(\frac{2ni}{r_1} - \tfrac{1}{2}n\pi - \tfrac{3}{4}\pi \right) \right] + \exp\left[-\mathrm{i}\left(\frac{2ni}{r_1} - \tfrac{1}{2}n\pi - \tfrac{3}{4}\pi \right) \right] \right\}, \tag{5.13}$$

and

$$g \approx \tilde{E} r_1^{-n+\frac{1}{2}} \left\{ \exp\left[\mathrm{i}\left(\frac{2ni}{r_1} - \frac{\pi}{2}\sqrt{(n^2+4)} - \tfrac{3}{4}\pi \right) \right] + \exp\left[-\mathrm{i}\left(\frac{2ni}{r_1} - \frac{\pi}{2}\sqrt{(n^2+4)} - \tfrac{3}{4}\pi \right) \right] \right\}, \tag{5.14}$$

where E, $\tilde{E}$ are constants.

There are four other solutions of each of the sixth-order systems in this region. They are viscous solutions; two of them are exponentially large as $s \to \infty$ and must therefore be discarded. The two exponentially small ones will match automatically with the solutions in region 3 which we now discuss.

5.3. *Region* 3: $s = O(\mu^{\frac{1}{6}})$

It is this region that contains most of the oscillations evident in the numerical solutions. The solution sought therein is of W.K.B. form and we write, in (5.1),

$$s = \mu^{\frac{1}{6}} x \tag{5.15}$$

and

$$G = \exp\left[\nu \int f \, \mathrm{d}x \right] (\tilde{G}_0 + \tilde{G}_1/\nu + o(\nu^{-1})), \quad K = \nu^2 \exp\left[\nu \int f \, \mathrm{d}x \right] (\tilde{K}_0 + \tilde{K}_1/\nu + o(\nu^{-1})), \tag{5.16}$$

$$\Lambda = \mu^{\frac{1}{3}} (\Gamma_0 + \Gamma_1/\nu + o(\nu^{-1})), \tag{5.17}$$

where $\nu = \mu^{\frac{1}{3}}$ and $\mu \gg 1$. For Γ_0 we take $\Gamma_0 = 3n^{\frac{2}{3}} \mathrm{e}^{\frac{5}{6}\mathrm{i}\pi}$ as in (5.7*a*); it emerges that Γ_0 is the same for all modes of the type sought and the eigenvalues are distinguished by a sequence of values of Γ_1. Substitution of (5.15)–(5.17) into (5.1) yields, successively, relations between $\tilde{K}_0$ and G_0, an equation for f and, after some calculation, a differential equation for $\tilde{G}_0$. These are

$$(\Gamma_0 + x^2 - \mathrm{i}f^2)\, \tilde{K}_0 + 2n\tilde{G}_0 = 0, \tag{5.18}$$

$$f(\Gamma_0 + x^2 - \mathrm{i}f^2) = \pm 2n, \tag{5.19}$$

$$2x(\mathrm{i}f^3 - n)\, \tilde{G}_0' + [3\mathrm{i}f^2 f' x + (2n+1)(\mathrm{i}f^3 - n) + fx^2 - \Gamma_1 x f^2]\, \tilde{G}_0 = 0, \tag{5.20}$$

PHILOSOPHICAL TRANSACTIONS OF THE ROYAL SOCIETY A MATHEMATICAL, PHYSICAL & ENGINEERING SCIENCES

where, to derive (5.20), the plus sign in (5.19) has been used. With the minus sign in (5.19) the sign of both f and Γ_1 in (5.20) must be changed.

We now define f_1, f_2 and f_3 to be the roots of (5.19) with the plus sign and h_1, h_2 and h_3 the roots of (5.19) with the minus sign when $\Gamma_0 = 3n^{\frac{2}{3}} e^{\frac{5}{6}i\pi}$; thus $h_1 = -f_1$, etc. We aim to show the consistency of assuming this value of Γ_0 and to determine Γ_1. To leading order the solution in (5.16) for G is given by

$$\tilde{G}_0 = \sum_{j=1}^{3} \tilde{F}_j(x) \exp\left[\nu \int_0^x f_j \, dx_1\right] + \sum_{j=1}^{3} \tilde{H}_j(x) \exp\left[\nu \int_0^x h_j \, dx_1\right], \tag{5.21}$$

where

$$\tilde{F}_1(x) = \frac{C_j}{x^{n+\frac{1}{2}}(if_j^3 - n)^{\frac{1}{2}}} \exp\left[\tfrac{1}{2}\Gamma_1 \int_{n^{\frac{1}{3}}3^{\frac{3}{4}}}^{x} \frac{f_j^2}{if_j^3 - n} dx_1 - \frac{1}{2}\int_{n^{\frac{1}{3}}3^{\frac{3}{4}}}^{x} \frac{f_j x_1}{if_j^3 - n} dx_1\right], \tag{5.22a}$$

$$\tilde{H}_j(x) = \frac{D_j}{x^{n+\frac{1}{2}}(ih_j^3 + n)^{\frac{1}{2}}} \exp\left[\tfrac{1}{2}\Gamma_1 \int_{n^{\frac{1}{3}}3^{\frac{3}{4}}}^{x} \frac{h_j^2}{ih_j^3 + n} dx_1 - \frac{1}{2}\int_{n^{\frac{1}{3}}3^{\frac{3}{4}}}^{x} \frac{h_j x_1}{ih_j^3 + n} dx_1\right]. \tag{5.22b}$$

In figure 16 we plot the real parts of $n^{-\frac{1}{3}}f_j$, $n^{-\frac{1}{3}}h_j$ as functions of $n^{-\frac{1}{3}}x$. For small x,

$$f_1, f_2 \approx -n^{\frac{1}{3}} e^{-\frac{1}{6}i\pi} \pm \frac{1}{\sqrt{3}} e^{-\frac{1}{4}i\pi} x, \tag{5.23a}$$

$$f_3 = 2n^{\frac{1}{3}} e^{\frac{1}{6}i\pi} + O(x^2), \tag{5.23b}$$

and for large x

$$f_1, f_2 = \pm x/\sqrt{2} + O(1), \quad f_3 \approx 2n/x^2. \tag{5.24a, b}$$

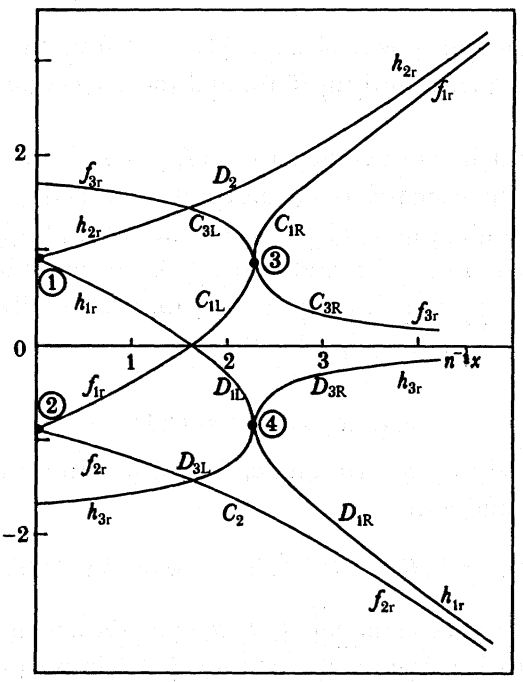

FIGURE 16. Real parts of $n^{-\frac{1}{3}}f_j$, $n^{-\frac{1}{3}}h_j$ in (5.21) as functions of $n^{-\frac{1}{3}}x$. The constants C_{1L}, C_{1R}, C_2, C_{3L}, C_{3R}, D_{1L}, D_{1R}, D_2, D_{3L}, D_{3R} in (5.22) are associated with the branches shown.

At $x = n^{\frac{1}{3}}3^{\frac{3}{4}}$ we have $f_1 = f_3$ (both real and imaginary parts) this being the reason for choosing it as the lower limit of integration in (5.22).

We aim to match this W.K.B. solution to the Bessel function solutions of region 1 as $x \to 0$ and $t \to \infty$, and to the Bessel functions of region 4 as $x \to \infty$ and $r_1 \to 0$. We shall match all six terms in (5.21), altering the direction of the path of integration when it is necessary to make the exponentially small terms determinate. We first note that the forms of f_j, h_j are, as $x \to 0$, exactly right to match the exponents in (5.9) because comparison of (5.19) and (5.5) shows that at $x = 0, f = -\mathrm{i}\tilde{p}$, and the relation between x and t is $\nu x = t$. Also, as $x \to \infty, f_3$ and h_3 are right to match the exponents in (5.13). Thus the solution in this region should bridge the gap between the two different Bessel function solutions, though additional regions will be required near $x = 0$ and $x = n^{\frac{1}{3}}3^{\frac{3}{4}}$ where two pairs of the exponents in (5.21) are equal. We see immediately from figure 16 that it will be necessary to set $D_2 = 0$ because of the exponential growth associated with h_2, and if we label the constants in (5.22) $C_{1\mathrm{L}}$, $C_{1\mathrm{R}}$, C_2, $C_{3\mathrm{L}}$, $C_{3\mathrm{R}}$, $D_{1\mathrm{L}}$, D_{1R}, $D_{3\mathrm{L}}$ and $D_{3\mathrm{R}}$, the L and R denoting that their values will differ each side of the point $x = n^{\frac{1}{3}}3^{\frac{3}{4}}$, then $C_{1\mathrm{R}}$ is also zero. It emerges that each of these constants is of the form $b_0 \mathrm{e}^{\nu c_0}$ where b_0, c_0 are, to leading order, independent of ν and it will be sufficient for our purpose to consider the exponents only; we shall write $\overset{\mathrm{e}}{=}$ to denote that two constants have equal exponents to leading order. Two relations between the exponents of the remaining eight constants follow at once. One follows from matching the terms in f_3 and h_3 to the term in A_3 in (5.9): we obtain

$$C_{3\mathrm{L}} \overset{\mathrm{e}}{=} D_{3\mathrm{L}} \overset{\mathrm{e}}{=} A_3. \tag{5.25}$$

Also for large x, the terms in h_3 and f_3 may be matched respectively to the two terms in (5.13) to give

$$E \overset{\mathrm{e}}{=} D_{3\mathrm{R}} \exp\left[\nu \int_0^\infty h_3 \,\mathrm{d}x\right] \overset{\mathrm{e}}{=} C_{3\mathrm{R}} \exp\left[\nu \int_0^\infty f_3 \,\mathrm{d}x\right]. \tag{5.26}$$

We may note the correct algebraic power of x, namely $x^{-n-\frac{1}{2}}$, from the match between the terms in f_3 and h_3 in (5.21) and the term in A_3 in (5.9), and the correct power, namely $x^{-n+\frac{1}{2}}$ for the match with (5.13).

An attempt at a direct match between the terms in f_1, f_2 and h_1 in (5.21) and those in A_1 and A_2 in (5.9) fails because of the mismatch of the algebraic powers of x and t. Thus an additional region is required in the neighbourhood of $x = 0$. The presence of this region is to be expected because of the equality of f_1 and f_2, and h_1 and h_2 at $x = 0$. The terms in f_3 and h_3 match straight through this region. It emerges that it is this region that essentially determines Γ_1, giving a sequence of values and corresponding eigenfunctions.

5.4. *Region* 2: $s = O(1)$

This region occurs because $f_1(0) = f_2(0)$ and $h_1(0) = h_2(0)$. In it the appropriate variable is s and we take $K = O(\nu^2 G)$ and write

$$G(s) = \mathrm{e}^{\nu\delta x} H(s) = \mathrm{e}^{\sqrt{\nu}\delta s} H(s), \quad K = \nu^2 \mathrm{e}^{\sqrt{\nu}\delta s} L(s), \tag{5.27}$$

where $\delta^6 = -n^2$ so that this will accommodate f_1, f_2, h_1 or h_2, the exponential factor $\mathrm{e}^{\nu\delta x}$ matching immediately with that in (5.21). We now substitute (5.27) into (5.1) and retain the leading terms and those of relative order $\nu^{-\frac{1}{2}}$ and ν^{-1}, because the two biggest sets of terms will go out

automatically as f_1 and h_1 are, at the origin, double roots of (5.19). After elimination of L and some calculation we find that the equation for H is

$$s^2H'' + (2n+1)\,sH' + [n^2 - \tfrac{1}{4} + \tfrac{1}{3}\mathrm{i}s^2(\Gamma_1 + s^2)]\,H = 0, \tag{5.28}$$

which, if we set,

$$s^2 = 3^{\frac{1}{3}}\,\mathrm{e}^{\frac{1}{4}\mathrm{i}\pi}z \quad \text{and} \quad H(s) = s^{\frac{1}{2}-n}\,\mathrm{e}^{-\frac{1}{2}z}\,S(z) \tag{5.29}$$

is recognizable as the confluent hypergeometric equation

$$zS'' + (\tfrac{3}{2} - z)\,S' - (\tfrac{3}{4} - \tfrac{1}{12}3^{\frac{1}{2}}\,\mathrm{e}^{\frac{3}{4}\mathrm{i}\pi}\Gamma_1)\,S = 0. \tag{5.30}$$

This is the equation that holds in the neighbourhood of both points ① and ② in figure 16. Near ① we take $\delta = n^{\frac{1}{3}}\,\mathrm{e}^{\frac{1}{6}\mathrm{i}\pi}$ in (5.27) and near ② we take $\delta = -n^{\frac{1}{3}}\,\mathrm{e}^{\frac{1}{6}\mathrm{i}\pi}$.

When s is small the solutions for H in (5.28) have $H \sim s^{-n+\frac{1}{2}}$, $s^{-n-\frac{1}{2}}$, which will match automatically with the powers of t_1 in (5.9). When $s \gg 1$

$$H(s) \approx \mathrm{e}^{\frac{1}{2}\delta_0 s^2}s^{-n-1-\mathrm{i}\Gamma_1/6\delta_0}, \tag{5.31}$$

where $\delta_0 = (1/\sqrt{3})\,\mathrm{e}^{-\frac{1}{4}\mathrm{i}\pi}$ for a match with the term in f_1 or h_2 in (5.21), and $\delta_0 = (-1/\sqrt{3})\,\mathrm{e}^{-\frac{1}{4}\mathrm{i}\pi}$ for a match with the term in f_2 or h_1. The powers of s in (5.31) match automatically with the powers of x as $x \to 0$ in the appropriate terms of (5.21).

In the neighbourhood of the point ① we must exclude the solution of (5.30) that is exponentially large as $z \to \infty$ because this would match with the term in h_2 in (5.21) which, by reference to figure 16, we noted above must not be present. Thus the required solution is, in the usual notation, $\Delta U(a_0, \frac{3}{2}, z)$, where

$$a_0 = \tfrac{3}{4} - (\tfrac{1}{12}3^{\frac{1}{2}})\,\mathrm{e}^{\frac{3}{4}\mathrm{i}\pi}\Gamma_1 \tag{5.32}$$

and Δ is a constant. We propose to match this solution, for $|s| \ll 1$, with the appropriate terms in (5.9), namely those in $\mathrm{e}^{\mathrm{i}\chi}$ (those in $\mathrm{e}^{-\mathrm{i}\chi}$ are matched at the point ②). Because, for small z,

$$U(a_0, \tfrac{3}{2}, z) \approx -\pi\left\{\frac{1}{(a_0 - \frac{3}{2})!\,\frac{1}{2}!} - \frac{1}{z^{\frac{1}{2}}(a_0 - 1)!\,(-\frac{1}{2})!}\right\}, \tag{5.33}$$

it follows from (5.29) that, for small s,

$$H(s) \approx -\pi^{\frac{1}{2}}\Delta s^{\frac{1}{2}-n}\left\{\frac{2}{(a_0 - \frac{3}{2})!} - \frac{1}{(a_0 - 1)!\,s(\sqrt{3}\mathrm{e}^{\frac{1}{4}\mathrm{i}\pi})^{\frac{1}{2}}}\right\}. \tag{5.34}$$

We note that the powers of s match automatically with the powers of t_1 in (5.9), and matching the constants, but again retaining the exponential factors only, leads to

$$\frac{\Delta}{(a_0 - \frac{3}{2})!} \overset{\mathrm{e}}{=} A_2, \quad \frac{\Delta}{(a_0 - 1)!} \overset{\mathrm{e}}{=} A_1 - \frac{4n^2+3}{8}A_2, \tag{5.35}$$

where it is essential to retain the factorials involving a_0, because it emerges that these, which determine the eigenvalue Γ_1, themselves have exponential factors.

When $|s| \gg 1$ we match this solution with the term involving h_1 in (5.21) as $x \to 0$. It may be verified, by using (5.22b) and the asymptotic form of $U(a_0, \frac{3}{2}, z)$ that the algebraic powers of s and x are exactly right (they involve Γ_1 in fact) and therefore that

$$\Delta \overset{\mathrm{e}}{=} D_{1\mathrm{L}}. \tag{5.36}$$

PHILOSOPHICAL TRANSACTIONS OF THE ROYAL SOCIETY A MATHEMATICAL, PHYSICAL & ENGINEERING SCIENCES

Near the point ② in figure 16 we require a solution of (5.30) that is exponentially large as $z \to \infty$ to give a match with the term in f_1 in (5.21). The constant C_2 would come from a match with the exponentially small component which would be determinate if we matched at an angle such that z were purely imaginary, i.e. $\arg s = \frac{3}{8}\pi$. However, the value of C_2 is immaterial because it corresponds to a solution of W.K.B. type that is exponentially small as $x \to \infty$. Thus we match only the exponentially large term as $s \to \infty$. The required solution of (5.30) leads to

$$H(s) = s^{\frac{1}{2}-n}\,\mathrm{e}^{-\frac{1}{2}z}[\alpha_0\,U(a_0, \tfrac{3}{2}, z) + \beta_0\,M(a_0, \tfrac{3}{2}, z)], \tag{5.37}$$

where α_0 and β_0 are constants. When $s \ll 1$, we have from (5.37) that

$$H(s) \approx s^{\frac{1}{2}-n}\left[\beta_0 - \frac{2\alpha_0\sqrt{\pi}}{(a_0-\frac{3}{2})!} + \frac{\alpha_0\sqrt{\pi}(\sqrt{3}\mathrm{e}^{\frac{1}{4}i\pi})^{\frac{1}{2}}}{(a_0-1)!\,s}\right], \tag{5.38a}$$

and for $s \gg 1$,

$$H(s) \approx \frac{\beta_0}{(a_0-1)!}\,s^{\frac{1}{2}-n}\left(\frac{s^2}{\sqrt{3}}\mathrm{e}^{-\frac{1}{4}i\pi}\right)^{a_0-\frac{3}{2}} \exp\left[\frac{s^2}{2\sqrt{3}}\mathrm{e}^{-\frac{1}{4}i\pi}\right]. \tag{5.38b}$$

Thus matching the exponential parts of the constants in (5.37) and (5.38) with the terms in e^{-ix} in (5.9) and the terms involving f_1 in (5.21) respectively we obtain

$$\beta_0 - \frac{2\alpha_0\sqrt{\pi}}{(a_0-\frac{3}{2})!} \overset{\mathrm{e}}{=} A_2, \quad \frac{\alpha_0}{(a_0-1)!} \overset{\mathrm{e}}{=} A_1 - \frac{4n^2+3}{8}A_2 \tag{5.39}$$

and

$$\frac{\beta_0}{(a_0-1)!} \overset{\mathrm{e}}{=} C_{1\mathrm{L}}. \tag{5.40}$$

The analysis of the neighbourhood of the point ① gave us A_1 in terms of A_2 (from (5.35)) as a result of excluding the term in h_2 in (5.21), and then $D_{1\mathrm{L}}$ in terms of them as in (5.36). This examination of the neighbourhood of the point ② has now given us $C_{1\mathrm{L}}$ in terms of A_1 and A_2 as

$$C_{1\mathrm{L}} \overset{\mathrm{e}}{=} \frac{A_2}{(a_0-1)!} + \frac{2\sqrt{\pi}}{(a_0-\frac{3}{2})!}\left(A_1 - \frac{4n^2+3}{8}A_2\right). \tag{5.41}$$

The interpretation of (5.41), from which are omitted multiplicative powers of ν and order one constants, is that at least two of the three terms $C_{1\mathrm{L}}$, $A_2/(a_0-1)!$ and

$$(A_1 - (4n^2+3)\,A_2/8)/(a_0-\tfrac{3}{2})!$$

have the same exponential constant factor. The third may be smaller.

5.5. *The regions* $x = n^{\frac{1}{3}}3^{\frac{3}{4}} + O(\nu^{-\frac{2}{3}})$

At the point marked ③ in figure 16 we have $f_1 = f_3$, and at ④ we have $h_1 = h_3$, so that these are turning points of the W.K.B. solution. To the right of ③ we must exclude the term with exponential growth, i.e. $C_{1\mathrm{R}} = 0$, and to the right of ④ we require the exponentially growing term in $D_{3\mathrm{R}}$ to match with the Bessel functions in region 4, and the value of the exponentially decaying term with factor $D_{1\mathrm{R}}$ is immaterial. The relation between $C_{3\mathrm{R}}$ and $D_{3\mathrm{R}}$ is given by (5.26).

We deal first with the point ③. It emerges that the appropriate equation in the neighbourhood of this point is Airy's equation and is found by setting

$$x = n^{\frac{1}{3}}3^{\frac{3}{4}} + \nu^{-\frac{2}{3}}X_1, \tag{5.42}$$

with $s = \mu^{\frac{1}{6}}x$ as in (5.15), in (5.1). As in the neighbourhood of ① and ②, and throughout the region $x = O(1)$, $K = O(\nu^2 G)$, and analogously to (5.27) we write

$$G(s) = \mathrm{e}^{\nu\delta x} H_2(X_1), \quad K(s) = \nu^2 \mathrm{e}^{\nu\delta x} L_2(X_1). \tag{5.43}$$

For this discussion of the point ③ we require $\delta = n^{\frac{1}{3}} \mathrm{e}^{-\frac{1}{6}\mathrm{i}\pi}$, i.e. the value of f_1 and f_3 at $x = n^{\frac{1}{3}}3^{\frac{3}{4}}$. In (5.1) we retain the leading-order terms and those of relative order $\nu^{-\frac{1}{3}}$ and $\nu^{-\frac{2}{3}}$. On elimination of L_2 the result is that H_2 satisfies

$$H_2'' + (\tfrac{2}{3})\,\mathrm{i}n^{\frac{1}{3}}3^{\frac{3}{4}} X_1 H_2 = 0 \tag{5.44}$$

with solutions Ai and Bi of argument

$$\left(\frac{2n^{\frac{1}{3}}}{3^{\frac{1}{4}}}\right)^{\frac{1}{3}} \mathrm{e}^{-\frac{1}{6}\mathrm{i}\pi} X_1. \tag{5.45}$$

Now to the right of the point ③ we must exclude the exponentially large term, i.e. we must have no multiple of the function Bi. To the left of ③, if X_1 is real then Ai is exponentially large for $X_1 \ll -1$ and the exponentially small contribution is, in the sense of Poincaré, indeterminate. As we wish to connect both $C_{1\mathrm{L}}$ and $C_{3\mathrm{L}}$ with $C_{3\mathrm{R}}$ we therefore choose to match with the solution (5.21) along a line on which $\mathrm{e}^{-\frac{1}{6}\mathrm{i}\pi} X_1$ is real. Thus, for $X_1 \mathrm{e}^{-\frac{1}{6}\mathrm{i}\pi} \ll -1$,

$$Ai\left(\left(\frac{2n^{\frac{1}{3}}}{3^{\frac{1}{4}}}\right)^{\frac{1}{3}} \mathrm{e}^{-\frac{1}{6}\mathrm{i}\pi} X_1\right) \propto (-X_1)^{-\frac{1}{4}} (\mathrm{e}^{\mathrm{i}(\xi+\frac{1}{4}\pi)} - \mathrm{e}^{-\mathrm{i}(\xi+\frac{1}{4}\pi)}), \tag{5.46}$$

where

$$\xi = \frac{2}{3}\left(\frac{2n^{\frac{1}{3}}}{3^{\frac{1}{4}}}\right)^{\frac{1}{2}} \mathrm{e}^{-\frac{1}{4}\mathrm{i}\pi} (-X_1)^{\frac{3}{2}}. \tag{5.47}$$

Now near the point ③ where $f_1 = f_3$ we have, for $x < n^{\frac{1}{3}}3^{\frac{3}{4}}$,

$$f_1, f_3 \approx n^{\frac{1}{3}} \mathrm{e}^{-\frac{1}{6}\mathrm{i}\pi} \pm \frac{2^{\frac{1}{2}} n^{\frac{1}{3}} \mathrm{e}^{-\frac{1}{4}\mathrm{i}\pi}}{3^{\frac{1}{8}}} (n^{\frac{1}{3}}3^{\frac{3}{4}} - x)^{\frac{1}{2}} \tag{5.48}$$

so that the exponents $\mathrm{e}^{\pm\mathrm{i}\xi}$ in (5.46) match with those in the terms in f_1 and f_3 in (5.21). The power $(-X_1)^{-\frac{1}{4}}$ is also correct, and matching the exponential part of the constant leads to

$$C_{3\mathrm{L}} \left[\nu \int_0^{n^{\frac{1}{3}}3^{\frac{3}{4}}} f_3 \,\mathrm{d}x\right] \overset{\mathrm{e}}{=} C_{1\mathrm{L}} \exp\left[\nu \int_0^{n^{\frac{1}{3}}3^{\frac{3}{4}}} f_1 \,\mathrm{d}x\right]. \tag{5.49}$$

For $\mathrm{e}^{-\frac{1}{6}\mathrm{i}\pi} X_1 \gg 1$, Ai is exponentially small as required, and again we may check that the exponent matches with that in the term in f_3 in (5.21) and that the $X_1^{-\frac{1}{4}}$ power is also correct. A match of the exponential parts of the constants gives

$$C_{3\mathrm{R}} \overset{\mathrm{e}}{=} C_{3\mathrm{L}}. \tag{5.50}$$

In the neighbourhood of the point ④ the analysis is similar, but this time we require a multiple of the solution Bi as well as of Ai. We again match with $X_1 \mathrm{e}^{-\frac{1}{6}\mathrm{i}\pi}$ real and obtain

$$D_{3\mathrm{R}} \exp\left[\nu \int_0^{n^{\frac{1}{3}}3^{\frac{3}{4}}} h_3 \,\mathrm{d}x\right] \overset{\mathrm{e}}{=} D_{1\mathrm{L}} \exp\left[\nu \int_0^{n^{\frac{1}{3}}3^{\frac{3}{4}}} h_1 \,\mathrm{d}x\right] + D_{3\mathrm{L}} \exp\left[\nu \int_0^{n^{\frac{1}{3}}3^{\frac{3}{4}}} h_3 \,\mathrm{d}x\right]. \tag{5.51}$$

No relation is found between D_{1L} and D_{3L} because, in contrast with the argument relevant to the point ④, we are not excluding an exponentially large term to the right of $x = n^{\frac{1}{3}}3^{\frac{3}{4}}$. The value of D_{1R} could be found if required but it is immaterial.

Thus we have nine relations between the exponential parts of the nine constants A_1, A_2, A_3, C_{1L}, C_{3L}, C_{3R}, D_{1L}, D_{3L} and D_{3R}. Essentially, setting the determinant of the coefficients to zero determines the one unknown a_0 which, from (5.32), then leads to Γ_1. Elimination between these relations, i.e. successive substitution in (5.25) and (5.26), and (5.35) and (5.37) for the D_s in terms of the C_s, and A_1 and A_2, and finding that the term in D_{3L} on the right-hand side of (5.51) is exponentially smaller than the other terms and may be ignored, gives finally

$$(a_0-\tfrac{3}{2})!\,A_2 \stackrel{e}{=} (a_0-1)!\,(A_1-\tfrac{1}{8}(4n^2+3)\,A_2) \tag{5.52}$$

together with

$$(a_0-1)!\,(a_0-\tfrac{3}{2})! \stackrel{e}{=} \exp\left[2\nu\int_0^\infty f_3\,\mathrm{d}x+2\nu\int_0^{n^{\frac{1}{3}}3^{\frac{3}{4}}}(f_1-f_3)\,\mathrm{d}x\right], \tag{5.53}$$

if either $A_2 \neq 0$ or $A_1-\frac{1}{8}A_2(4n^2+3) \neq 0$. The real part of the integral on the right-hand side of (5.53) has been evaluated as

$$\mathrm{Re}\left[\int_0^\infty f_3\,\mathrm{d}x+\int_0^{n^{\frac{1}{3}}3^{\frac{3}{4}}}(f_1-f_3)\,\mathrm{d}x\right] = (4.36-4.04)\,n^{\frac{2}{3}} > 0. \tag{5.54}$$

Thus the right-hand side of (5.53) is exponentially large and to balance it we must have $(a_0-\frac{3}{2})!$ or $(a_0-1)!$ to be infinite. Hence either

$$a_0 = \tfrac{1}{2}, -\tfrac{1}{2}, -\tfrac{3}{2}, \ldots \quad \text{with} \quad A_2 = 0, A_1 \neq 0 \tag{5.55}$$

or

$$a_0 = 0, -1, -2, \ldots \quad \text{with} \quad A_1 = \tfrac{1}{8}(4n^2+3)\,A_2, A_2 \neq 0. \tag{5.56}$$

We now therefore have a doubly infinite sequence of values of a_0 and hence of eigenvalues Γ_1. The leading one has $a_0 = \frac{1}{2}$ so that

$$\Lambda = 3\mu^{\frac{1}{3}}n^{\frac{2}{3}}\,\mathrm{e}^{\frac{5}{6}i\pi}+\sqrt{3}\,\mathrm{e}^{-\frac{3}{4}i\pi}+o(1). \tag{5.57}$$

For the second one $a_0 = 0$ and

$$\Lambda = 3\mu^{\frac{1}{3}}n^{\frac{2}{3}}\,\mathrm{e}^{\frac{5}{6}i\pi}+3\sqrt{3}\,\mathrm{e}^{-\frac{3}{4}i\pi}+o(1). \tag{5.58}$$

The fundamental assumption of the above argument is that the required value of Γ_0 is such that (5.19) has equal roots for f at $x = 0$. If this assumption is not made then it is not necessary to consider the region $s = O(1)$, and the match between the W.K.B. solution and the Bessel functions in the region $s = O(\mu^{-\frac{1}{6}})$ is, to leading order, independent of the eigenvalue. Thus it seems that the determinant of coefficients cannot be made to vanish and only the trivial solution results. We shall see in §7 that the agreement between the results of this section and those of the numerical work described in §3.4 is very good which gives us confidence that the argument is correct. However, we first show that, apart from the region where $s = O(\sigma^{\frac{1}{2}})$, discussed in §5.2, the same analysis holds for (4.16), and that the values of λ may be obtained by writing σ for μ in (5.57) and (5.58) and so on for the higher modes.

6. The identification of λ and σ with Λ and μ for the oscillatory eigensolutions

The numerical study of §4 strongly indicates that as μ and σ become large the values of Λ in (3.32) and those of λ in (4.16) are the same, i.e. $\Lambda(\mu) \approx \lambda(\sigma)$. Indeed $G(s) \approx g(s)$ as may be seen by comparing figures 6*a* and 13 for $n = 1$, $\mu = \sigma = 400$, figures 7*a* and 14 for $n = 1$, $\mu = \sigma = 800$ and figures 8*a* and 14 for $n = 2$, $\mu = \sigma = 400$. To demonstrate that the limiting form is the same it is necessary to eliminate K from (3.32) (or equivalently from (5.1)) and h from (4.16).

On substituting for K from (5.1*a*) into (5.1*b*) and defining

$$k_G(s,\Lambda) = -4s^2G/n + (s/2n)(\Lambda+s^2)(sG''+(2n+1)G') - (\mathrm{i}/2n) \times [s^2G^{\mathrm{IV}} + (4n+2)sG''' + (4n^2-1)G'' - (4n^2-1)G'/s], \quad (6.1)$$

we find that the equation for $G(s)$ reduces to

$$(\Lambda+s^2)(k_G - 4s^2G/n) - 2n\mu s^2G = \mathrm{i}[k_G'' + (2n-3)k_G'/s - 4(n-1)k_G/s^2 + (6s^2/n)G'' + (6/n)(2n+1)sG']. \quad (6.2)$$

To eliminate h from (4.16) it is simpler first to define

$$h = -g - (s/n)g' + \tilde{h} \quad (6.3)$$

whereupon (4.16*a*) becomes

$$ns(\lambda+s^2)\tilde{h} - 2s^3g = \mathrm{i}n[s\tilde{h}'' + (2n-3)\tilde{h}' - 4(n-1)\tilde{h}/s]. \quad (6.4)$$

When the substitution (6.3) is made in (4.16*b*) it may be written as, after use of (6.4) which enables the derivatives of $\tilde{h}$ to be eliminated,

$$s^2(\lambda+s^2)(sg''+(2n+1)g') - 8s^3g = 2ns(n^2\sigma - \lambda - s^2)\tilde{h} - \mathrm{i}[s^3g^{\mathrm{iv}} + (4n+2)s^2g''' + (4n^2-1)sg'' - (4n^2-1)g']. \quad (6.5)$$

Thus we may solve for $\tilde{h}$ as

$$\tilde{h} = k_g(s,\lambda)/(n^2\sigma - \lambda - s^2), \quad (6.6)$$

and upon substitution into (6.4) the equation for k_g is

$$(\lambda+s^2)\left(k_g + \frac{2s^2g}{n}\right) - 2n\sigma s^2g = \mathrm{i}\left[k_g'' + (2n-3)k_g'/s - 4(n-1)k_g/s^2 + 4\left(sk_g' + (n-1)k_g + \frac{2s^2k_g}{n^2\sigma - \lambda - s^2}\right)\Big/(n^2\sigma - \lambda - s^2)\right]. \quad (6.7)$$

It is clear that (6.2) and (6.7) have, apart from one term, corresponding left-hand sides, and also have the first three terms corresponding on the right-hand sides. To show that, to leading order for $\mu \gg 1$, $\sigma \gg 1$, the functions g, G are such that $g(s) \approx G(s)$, apart from in the regions where $s = O(\mu^{\frac{1}{4}})$ and $s = O(\sigma^{\frac{1}{4}})$, it is necessary to verify that the analysis of §5 does not use the non-common terms to obtain Λ and λ to $O(1)$. This verification has been undertaken. In the very outer region the orders of the Bessel functions for the two problems are different as shown in (5.11) and (5.12) because the algebraic decay differs; this difference in algebraic decay may

be detected in figures 7*a* and 14 for example. In the very outer region the appropriate inviscid equations to be solved are obtained by setting $\Lambda = 0 = \lambda$ in (6.2) and (6.7), and by neglecting the terms multiplied by i throughout. It may be noted that, with $\lambda = O(\sigma^{\frac{1}{3}})$, (6.7) has a singular point in the region where $s = O(\sigma^{\frac{1}{2}})$; however, the leading approximation, given by (5.12), is regular.

It follows therefore that these highly oscillatory viscous modes occur, when the Reynolds number is sufficiently large, right across the unstable region between the neutral curves of Cotton & Salwen (1981) in the (R, Ω)-plane. They are not simply confined to the neighbourhoods of the neutral curves themselves.

7. A comparison between the numerical work of §4 and the analysis of §5

It remains to demonstrate, as convincingly as possible, that the modes described in §5 are indeed being attained by the numerical solutions of (3.32) and (4.16) as μ and σ respectively become large. The modes that become inviscid as μ and $\sigma \to \infty$, i.e. when $n = 1$ the second mode in the μ-problem and the third in the σ-problem, and when $n = 2$ the third in the μ-problem and the fourth in the σ-problem, seem to be an anomaly and are in any case not the most important.

To begin with we undertake a qualitative comparison and then quantify the statements made. Firstly there is the assumption that the oscillation is concentrated in the part of the region where $s = O(\mu^{\frac{1}{3}})$ (for the second problem replace μ by σ). When $\mu = 400$, if $s^2 = \mu^{\frac{1}{3}}$ then $\zeta = \ln(s^2+1) = 2.12$, and if $\mu = 800$ then $\zeta = 2.33$, which are not inconsistent with the regions of high oscillation in figures 6–8 and 13–15. That the number of oscillations, at say $\mu = 800$, is still small, of the order of two or three, is a reflection of the fact that the appropriate parameter is $\mu^{\frac{1}{3}}$ and still therefore modest. It is thus felt not to be significant that the oscillations do not yet extend quite as far as $s = n^{\frac{1}{3}}3^{\frac{3}{4}}\mu^{\frac{1}{6}}$. In addition, these wildly oscillatory eigenfunctions are not easy to compute though fortunately the eigenvalue is invariably of greater accuracy.

A second visual check may be made that verifies the assumption $K = O(\mu^{\frac{2}{3}}G)$ when $s = O(\mu^{\frac{1}{6}})$ and smaller. From figures 6*b*, 7*b* and 8*b* we see that this is also reasonable. A notable feature of figure 2 is the parallelism of the curves labelled $p = 0$ and 2 for μ greater than about 120. A similar remarks holds for those labelled $p = 1$ and 2 'second branch' (both for $\mu > 0$ and for $\mu < 0$) and for those labelled $p = 0$, 1 and 3 for $\mu > 0$ in figure 3. For the second problem a similar phenomenon is evident for those labelled 1, 2 and 4 in figure 10 and 1, 2, 3 and 5 in figure 11 when $\sigma > 0$. When $\sigma < 0$ the curves, including those numbered 3 and 4 in the respective diagrams, are again almost parallel. We may note that the values of a_0 proposed in (5.55) and (5.56) lead, from (5.2), (5.17) and (5.32) to

$$\Lambda = 3\mu^{\frac{1}{3}}n^{\frac{2}{3}}\mathrm{e}^{\frac{5}{6}\mathrm{i}\pi} + \sqrt{3}(1+2I)\,\mathrm{e}^{-\frac{3}{4}\mathrm{i}\pi} + o(1), \quad I = 0, 1, 2, \ldots, \tag{7.1}$$

so that the distance between successive eigenvalues is $-\sqrt{6}(1+\mathrm{i})$ which, in addition, is independent of n. It can be seen that the distance between the parallel curves is approximately $\sqrt{6}$.

The analysis starting with $p_1 = -n^{\frac{1}{3}}$ as in (5.7*c*) has not been carried through, though it may be conjectured that the values of a_0 are the same as in (5.54) which would account for the difference in the eigenvalues shown as 'second branch' for $p = 1$ and 2 in figure 2 also being

approximately $-\sqrt{6}(1+\mathrm{i})$. On the left, i.e. for $\mu \ll -1$ in figure 2, the second branch curves seem to be given by the value of p_1 in (5.7*b*); because $\mu < 0$ both Λ_i and Λ_r are negative.

A more precise comparison between the theory and the numerical results will now be presented. We first attempt to verify (7.1), remembering that the same formula holds for λ as a function of σ. In table 2 we tabulate

$$\bar{\Lambda}(n, I) \equiv \{\Lambda + \sqrt{\tfrac{3}{2}}(1+2I)\,(1+\mathrm{i})\}\, n^{-\frac{2}{3}}\mu^{-\frac{1}{3}}, \tag{7.2}$$

(where the values of Λ are obtained from the numerical work for the two most unstable modes for $\mu > 0$) for $I = 0, 1$ with $n = 1, 2$, and the correspondingly defined $\bar{\lambda}(n, I)$ in table 3. In each

TABLE 2. VALUES OF $\bar{\Lambda}$ AS DEFINED IN (7.2)

μ	$\bar{\Lambda}(1,0)$	$\bar{\Lambda}(1,1)$	$\bar{\Lambda}(2,0)$	$\bar{\Lambda}(2,1)$
100	−2.559+1.427i	−2.596+1.431i	−2.552+1.425i	−2.542+1.424i
200	−2.559+1.477i	−2.560+1.462i	−2.569+1.453i	−2.567+1.452i
300	−2.557+1.493i	−2.576+1.455i	−2.576+1.464i	−2.576+1.461i
400	−2.584+1.473i	−2.576+1.470i	−2.580+1.470i	−2.581+1.471i
500	−2.582+1.478i	−2.583+1.474i	−2.583+1.475i	−2.584+1.476i
600	−2.583+1.481i	−2.583+1.475i	−2.584+1.478i	
700	−2.583+1.483i	−2.585+1.479i	−2.586+1.480i	
800	−2.584+1.485i	−2.587+1.481i	−2.587+1.481i	
900	−2.585+1.486i		−2.588+1.483i	
1000	−2.585+1.488i		−2.589+1.484i	

TABLE 3. VALUES OF $\bar{\lambda}$ OBTAINED BY REPLACING Λ BY λ AND μ BY σ IN (7.2)

σ	$\bar{\lambda}(1,0)$	$\bar{\lambda}(1,1)$	$\bar{\lambda}(2,0)$	$\bar{\lambda}(2,1)$
100	−2.549+1.430i	−2.515+1.386i	−2.551+1.422i	−2.544+1.415i
200	−2.572+1.454i	−2.578+1.442i	−2.569+1.452i	−2.566+1.449i
300	−2.578+1.467i		−2.576+1.464i	
400	−2.582+1.472i		−2.580+1.470i	
500	−2.584+1.476i			
600	−2.585+1.479i			
700	−2.587+1.481i			
800	−2.587+1.483i			
900	−2.588+1.484i			
1000	−2.589+1.485i			

case the predicted limit as μ or σ tends to infinity is $3\mathrm{e}^{\frac{2}{3}\mathrm{i}\pi}$, i.e. $-2.598+1.5\mathrm{i}$. In addition to these comparisons on the eigenvalues it is instructive to make a comparison on the limiting eigenfunctions predicted in §6. For the leading eigenfunction we take, as suggested by (5.55), $A_2 = 0$ and $A_1 \neq 0$ in the inner solution (5.8); it may be shown, by using (5.25) and the other results of §5, that A_3 is also exponentially small. Thus, from (5.6) and (5.8) we obtain the result

$$K(0) \approx \mu^{\frac{2}{3}} n^{\frac{1}{3}} \mathrm{e}^{\frac{1}{3}\mathrm{i}\pi} = \mu^{\frac{2}{3}} n^{\frac{1}{3}} (0.866 + 0.5\mathrm{i}), \tag{7.3}$$

because $G(0) = 1$. In table 4 we show $K(0)/\mu^{\frac{2}{3}}n^{\frac{1}{3}}$ as derived from the numerical solution of (3.32) for the leading modes when $n = 1$, 2 and 3 for various values of μ. It seems that the asymptote predicted in (7.3) is being attained.

One further check is presented in table 5. This concerns the eigenfunction for the leading

TABLE 4. VALUES OF $K(0)/\mu^{\frac{2}{3}}n^{\frac{1}{3}}$ FOR $n = 1$, 2 AND 3

μ	$n=1$ $K(0)/\mu^{\frac{2}{3}}$	$n=2$ $K(0)/\mu^{\frac{2}{3}}2^{\frac{1}{3}}$	$n=3$ $K(0)/\mu^{\frac{2}{3}}3^{\frac{1}{3}}$
500	0.836+0.564i	0.830+0.573i	0.820+0.596i
600	0.839+0.543i	0.832+0.568i	0.822+0.588i
700	0.841+0.541i	0.834+0.565i	0.823+0.584i
800	0.843+0.539i	0.836+0.562i	
900	0.844+0.538i	0.836+0.559i	
1000	0.845+0.536i	0.837+0.557i	

TABLE 5. VALUES OF $\sigma^{-\frac{1}{3}}(\mathrm{d}h/\mathrm{d}\zeta+3\mathrm{d}g/\mathrm{d}\zeta)$ AT $\zeta = 0$ AS OBTAINED FROM THE NUMERICAL INTEGRATION

σ	$\sigma^{-\frac{1}{3}}(\mathrm{d}h/\mathrm{d}\zeta+3\mathrm{d}g/\mathrm{d}\zeta)_{\zeta=0}$
100	−0.839−0.582i
200	−0.845−0.564i
300	−0.852−0.554i
400	−0.855−0.549i
500	−0.856−0.546i
600	−0.858−0.542i
700	−0.860−0.541i
800	−0.862−0.538i
900	−0.863−0.536i
1000	−0.864−0.534i

mode of the σ-problem with $n = 1$. When $s = O(\sigma^{-\frac{1}{6}})$, i.e. $t = O(1)$, the limiting solution for g is the same as for $\tilde{G}$ in (5.8). Thus with $A_2 = A_3 = 0$ and $n = 1$

$$g \approx A_1 J_1(p_1 t)/p_1 t \tag{7.4}$$

and it may be shown that the corresponding function h is

$$h = -s\,\mathrm{d}g/\mathrm{d}s - g - A_1 \sigma^{-\frac{2}{3}} \mathrm{i} t J_1(p_1 t) \tag{7.5}$$

where $s = \sigma^{-\frac{1}{6}}t$ and $p_1 = \mathrm{e}^{-\frac{1}{3}\mathrm{i}\pi}$ as in (5.7a). Using this we may derive the relation

$$\mathrm{d}h/\mathrm{d}\zeta + 3\,\mathrm{d}g/\mathrm{d}\zeta = -\sigma^{-\frac{1}{3}}\mathrm{i}p_1 = -\sigma^{-\frac{1}{3}}(0.866+0.5\mathrm{i}) \tag{7.6}$$

between the derivatives of h and g with respect to ζ evaluated at $\zeta = 0$. The variable ζ, defined by $s^2 = \mathrm{e}^{\zeta} - 1$ as in (3.30), was used as independent variable for the numerical integration of (4.16). In table 5 we tabulate $\sigma^{-\frac{1}{3}}(\mathrm{d}h/\mathrm{d}\zeta+3\mathrm{d}g/\mathrm{d}\zeta)_0$ as derived from the numerical integration for the leading mode of (4.16), the predicted asymptote of which is displayed in (7.6). This, because it involves the derivatives of the calculated functions, is quite a stringent test of the agreement between the numerical work and the asymptotic analysis.

8. CONCLUSIONS

We have examined the centre modes of rotating Poiseuille flow that were recognized by Cotton & Salwen (1981) in their numerical computations as the Reynolds number R increases. These centre modes occur in the neighbourhoods of both the upper and lower branches of their neutral curves in the (R, Ω)-plane and have been shown here to satisfy limit equations containing parameters μ and σ respectively. As $|\mu|$ and $|\sigma| \to \infty$ possible solutions of the limit equations are the inviscid near-neutral centre modes discussed by Stewartson & Brown (1984).

Comparison with the data of C.S. taken at various large values of R confirms that the modes they obtained are indeed centre modes, and that the scaling and parameters of the limit equations are correct, but that the inviscid centre modes are not the attained asymptote on the unstable side of the neutral curve. Solutions of the limit equations at finite but large μ and σ show that the inviscid mode is a possible asymptote; for example when the azimuthal wavenumber $n = 1$ the inviscid asymptote is attained by the mode that at $\mu = 0$ is the second most unstable; but in general the large μ and σ solutions are *viscous*. We have analysed the form of these highly unstable viscous modes for $|\mu|$ and $|\sigma| \gg 1$ and the results are in good agreement, not only with the predictions of C.S., but also with the present solutions of the limit equations for finite μ and σ. It emerges that the solutions for both problems are the same when μ and σ respectively are sufficiently large, the implication of this being that these oscillatory viscous modes are present, as $R \to \infty$, right across the unstable region between the neutral curves. This is in accord with the results of C.S. who also predicted instability in this parameter range. A formula for ω for the region between the neutral curves may be written down from (3.2) and (5.57) (or equivalently from (4.2), (4.3) and (5.57) with Λ and μ replaced by λ and σ); this is

$$\omega \approx \alpha\epsilon - n + 3(\alpha^2\epsilon/R)^{\frac{1}{3}} e^{\frac{2}{3}i\pi}, \tag{8.1}$$

the conditions for the validity of which are $\epsilon n \gg \alpha$ and $\epsilon^2 \gg R$.

The modes described here are quite different in structure from the wall modes of Maslowe & Stewartson (1982) and the modes analysed by Pedley (1968, 1969). The inviscid modes studied by Maslowe & Stewartson are near-neutral with a critical layer on the wall of the pipe and are the limits as $n \to \infty$ of those earlier computed by Maslowe (1974). Even as n increases C.S. do not encounter such modes although they have larger growth rates than the inviscid centre modes of Stewartson & Brown (1984). When $R \gg 1$ the condition for the validity of the modes of Pedley (1968) is $\alpha^2/n^2 \ll 1$, $\alpha\epsilon^2 \ll \epsilon n - \alpha$ and, because it is possible to scale α out of the governing equations (2.2) so that this parameter appears only in the boundary condition which must now be applied at $r = \alpha$, one might expect that these modes for narrow tubes would bridge the gap between the theories of the wall modes and the centre modes. To a certain extent this interpretation is valid, as described by Stewartson & Brown. It is interesting that all these limiting theories predict $\epsilon n \approx \alpha$ as a neutral condition; the viscous theory of Pedley (1969) leads, in addition, to a second branch for the neutral curve that is in good agreement with the calculations of C.S. at the lower values of α, but the second branch for the wall modes of Maslowe & Stewartson is at $2\epsilon\alpha \approx n$. C.S. do not encounter this neutral curve, which would be another straight line in their (R, Ω)-plane but of very small slope at large R. However, as the dominant modes are likely to be the viscous centre modes that we have described here, it is not surprising that a numerical method tuned to capture these does not reveal the near-neutral inviscid wall modes.

A final comment concerns the application of the study to other vortex flows. Inviscid centre modes are known to exist for the trailing-line vortex of Lessen *et al.* (1974) if the swirl is not too large. Stewartson (1982), in an analysis for $n \gg 1$, showed that the ring modes of Leibovich & Stewartson (1983) are stabilized by viscosity in that the amount of swirl required for stability is less. The effect of viscosity on the centre modes of Stewartson & Brown (1985) has not yet been examined (the studies by Lessen & Paillet 1974 are at moderate values of the Reynolds number) although it would be of interest to examine the possibility of viscous centre modes in that situation also. These may be unstable at all values of the swirl.

PHILOSOPHICAL TRANSACTIONS OF THE ROYAL SOCIETY A MATHEMATICAL, PHYSICAL & ENGINEERING SCIENCES

This work was initiated before the death of Keith Stewartson, in May 1983. We hope that it has been completed as he would have wished and accept responsibility for any misconceptions or errors. K.S. and S.N.B. benefited from support from the Fluid Mechanics Program of the National Science Foundation under Grant MEA 8306713, and T.W.N. is indebted to the Science and Engineering Research Council for a research assistantship. We are grateful to Stephen Cowley for advice and encouragement and to Professor Harold Salwen for the generous provision of unpublished data.

References

Batchelor, G. K. & Gill, A. E. 1962 *J. Fluid Mech.* **14**, 529–551.
Berry, P. E. & Norbury, J. 1985 Technical report TPRD/M/1527/R85, Central Electricity Generating Board.
Cotton, F. W. & Salwen, H. 1981 *J. Fluid Mech.* **108**, 101–125.
Drazin, P. G. & Reid, W. 1981 *Hydrodynamic stability*. Cambridge University Press.
Howard, L. N. & Gupta, A. S. 1962 *J. Fluid Mech.* **14**, 463–476.
Leibovich, S., Brown, S. N. & Patel, Y. 1986 *J. Fluid Mech.* **173**, 595–624.
Leibovich, S. & Stewartson, K. 1983 *J. Fluid Mech.* **126**, 335–356.
Lessen, M. & Paillet, F. 1974 *J. Fluid Mech.* **65**, 769–779.
Lessen, M., Singh, P. J. & Paillet, F. 1974 *J. Fluid Mech.* **63**, 753–763.
Mackrodt, P. A. 1976 *J. Fluid Mech.* **73**, 153–164.
Maslowe, S. A. 1974 *J. Fluid Mech.* **64**, 307–317.
Maslowe, S. A. & Stewartson, K. 1982 *Physics Fluids* **25**, 1517–1523.
Pedley, T. J. 1968 *J. Fluid Mech.* **31**, 603–607.
Pedley, T. J. 1969 *J. Fluid Mech.* **35**, 97–115.
Stewartson, K. 1982 *Physics Fluids* **25**, 1953–1958.
Stewartson, K. & Brown, S. N. 1984 *IMA J. appl. Math.* **32**, 311–333.
Stewartson, K. & Brown, S. N. 1985 *J. Fluid Mech.* **156**, 387–399.
Stewartson, K. & Capell, K. 1985 *J. Fluid Mech.* **156**, 369–386.
Stewartson, K. & Leibovich, S. 1987 *J. Fluid Mech.* **178**, 549–566.

PHILOSOPHICAL TRANSACTIONS OF THE ROYAL SOCIETY A MATHEMATICAL, PHYSICAL & ENGINEERING SCIENCES